

Revisiting Chronology Protection Conjecture in The Dyonic Kerr-Sen Black Hole Spacetime

Teephatai Bunyaratavej,^{1,*} Piyabut Burikham,^{1,†} and David Senjaya^{1,‡}

¹*High Energy Physics Theory Group, Department of Physics,
Faculty of Science, Chulalongkorn University, Bangkok 10330, Thailand,*

(Dated: August 27, 2024)

The Chronology Protection Conjecture (CPC) was first introduced by Hawking after his semi-classical investigation to the behaviour of a spacetime with closed timelike curves (CTCs) in response to scalar perturbation. It is argued that there would be instabilities leading to amplification of the perturbation and finally causing collapse of the region with CTCs. In this work, we investigate the CPC by exactly solve the Klein-Gordon equation in the region inside the inner horizon of the non-extremal Dyonic Kerr-Sen (KS) black hole, where closed timelike curves exist. Successfully find the exact radial solution, we apply the polynomial condition that turns into rule of the energy quantization. The quasinormal modes (QNMs) of the scalar fields in the region inside the inner horizon of the rotating black hole with nonzero energy have only positive imaginary part describing states that grow in time. The exponentially growing modes will backreact and deform the spacetime region where CTC exists. The CPC is proven to be valid in the Dyonic Kerr-Sen black hole spacetime. Moreover, since the Dyonic Kerr-Sen black hole is the most general axisymmetric black hole solution of the string inspired Einstein-Maxwell-dilaton-axion (EMDA) theory, the semiclassical proof in this work is also valid for all simpler rotating black holes of the EMDA theory. The structure of the Dyonic KS spacetime distinctive from the Kerr-Newman counterpart is also explored.

I. INTRODUCTION

Investigation of various types of quantum fields in exterior black hole (BH) spacetimes has been a booming research in the last decades. The explorations have uncovered numerous fascinating facets of quantum field theories in relation with black hole physics. One of the examples is the quasinormal ringing that embodies unique black hole's parameters that reverberates over spacetime when a black hole is perturbed. The quantized oscillation frequencies are termed quasinormal modes instead of normal modes, given their complex valued nature. The real component of a mode indicates the oscillation frequency, while the imaginary part signifies the damping or grows. These complex modes are important unique frequencies and directly relate to the black hole's parameters, i.e., mass, angular momentum and charges.

After the groundbreaking detection of a binary black hole merger's gravitational wave signal on September 14, 2015, the Hawking radiation from an optical black hole analog was recently observed [1–3]. This marks the emergence of black hole spectroscopy as a significant area of interest in physics. Quasibound states, quasinormal modes, and shadows of black holes are intriguing features of these cosmic entities, manifesting in observable spectra as particles enter the black hole. The importance of finding the exact solutions of the governing Klein-Gordon equation which describes the relativistic quantum mechanics of scalar fields in a given curved spacetime is that

it will allow us to analytically investigate not only exact black hole's quasinormal modes, but also the black hole's horizon thermodynamics that constitutes the first substantial step to understand the quantum field theory in curved spacetime. This is in contrast to the widely used WKB approximation, where the approximation breaks down for low valued momentum, $p = \hbar k \approx 0$, and the approximated wave function breaks down near potential barriers [53, 54].

Nonetheless, the study of how relativistic fields behave in the black hole's interior spacetime has only started to gain attention relatively recently [4–7]. One of primary justifications on the significance of the investigation of the Dyonic Kerr-Sen black hole's inner region is to verify the Chronology Protection Conjecture (CPC). Since the Dyonic Kerr-Sen black hole is the most general axisymmetric black hole solution that incorporates all other axisymmetric black hole solutions such as Kerr and Kerr-Sen also their axionic and dilatonic versions [8–11], verifying the CPC in the Dyonic Kerr-Sen spacetime is automatically verifying CPC in the other simpler axisymmetric black hole solutions. Dyonic KS spacetime also has very rich spacetime structure [12, 13], many aspects of which do not exist in General Relativity counterpart, the Kerr-Newman spacetime. It is interesting to explore the differences with respect to CTC and singularity behaviour.

The term “CPC” was encoded by Hawking in 1992 by employing a semi-classical investigation of the stress tensor in the wormhole throat [14]. The conjecture argues that there exists a physical mechanism capable of averting the formation of closed timelike curves, that the region inside the inner horizon of rotating black holes with CTCs exhibit instability, i.e., particles or fields entering the aforementioned region will experience repeating

* teephatai@gmail.com

† piyabut@gmail.com

‡ davidsenjaya@protonmail.com

blueshift proportional to the winding number of trajectory around the CTC region. In Hawking's investigation [14] of a radiation beam entering one end of a wormhole while considering vacuum fluctuations, it reveals that the beam would naturally realign itself before reaching the opposite end of the wormhole. This phenomenon implies that the accumulation of radiation becomes sufficiently significant to cause the collapse of the wormhole. The investigation in Ref. [15, 16] reveals that perturbation of relativistic boson fields to a wormhole throat will cause bifurcation of horizons and either explodes to form an inflationary universe or collapses to a black hole depending on the total input energy, respectively, negative or positive. However, uncertainty still surrounded Hawking's conclusion as semi-classical quantum field theory in curved space is not reliable for high energy densities or brief time intervals close to the Planck scale with non-negligible backreaction to the spacetime, necessitating a comprehensive theory of quantum gravity for precise verdict [17].

On the other hand, the CTC also exists behind the Cauchy horizon of the charged rotating BH in General Relativity, the Kerr-Newman spacetime. It was argued that these CTCs, even exist, are safe since it is hidden by the Cauchy horizon. In this work, we consider CPC of the KSBH by studying the behaviour of test scalar fields in the black hole's region inside the inner horizon in fully relativistic quantum description. Firstly, the Klein-Gordon equation in the Dyonic Kerr-Sen black hole background is constructed. We then apply the separation ansatz to separate the radial part. Following the recent developments of the Heun-family special functions and their applications as novel exact solutions of the Klein-Gordon's radial equation in various black hole backgrounds [18–26], in this work, we present exact solutions of the scalar fields in the Dyonic Kerr-Sen black hole's interior region in terms of the Confluent Heun functions. From the polynomial condition, we obtain energy quantization condition. By applying appropriate boundary conditions for the QNMs, we find that in the region with the CTC, outgoing massive and massless scalar fields in the analytically continued spacetime are unstable, characterized by having positive imaginary part of the quantized energy, leading to the exponential growth in time. For massless case, with exact explicit formula of the QNMs, we can show that all nonzero-energy modes are unstable and exponentially growing in time. Inevitably, this leads to the ever increasing backreaction to the spacetime region behind the inner horizon, and destroy the spacetime region where the presence of CTC is allowed.

This work is presented as follows. In Section II, we review the Dyonic Kerr-Sen black hole's classical properties, i.e., the metric, horizons, singularities. In Section III, we discuss the closed timelike curve. The contour plots of the CTCs and the metric functions for various scenarios of the Dyonic KSBH's parameters are presented. Detail derivations to obtain the exact radial solutions of the governing Klein-Gordon equation and the

quantized energy levels for both massive and massless scalar fields are presented in Section IV and V. Graphical visualizations of the complex quasiresonance frequencies for all massive modes are also shown. Growing QNMs with specific boundary conditions are demonstrated to exist in Section V C. We argue that they validate the CPC. Section VI concludes our work.

II. THE DYONIC KERR-SEN BLACK HOLE

The Dyonic Kerr-Sen black hole is the most general axisymmetric black hole solution of the string inspired Einstein-Maxwell-dilaton-axion (EMDA) theory of gravity, where the generalization of the Einstein-Maxwell sector is done by introducing coupling between the Maxwell electromagnetic field tensor $F_{\mu\nu}$ with the the scalar dilaton field ξ and introducing the pseudo scalar axion field ϕ coupled to the dilaton field ξ . The theory is given by this following effective action defined in 3+1 dimension spacetime [27, 28],

$$S_{EMDA} = \frac{1}{16\pi} \int [R - 2\partial_\mu \xi \partial^\mu \xi - \frac{1}{3} H_{\rho\sigma\delta} H^{\rho\sigma\delta} + e^{-2\xi} F_{\alpha\beta} F^{\alpha\beta}] \sqrt{-g} d^4x, \quad (1)$$

where R is the Ricci scalar and g is the metric tensor determinant. The Maxwell electromagnetic field tensor $F_{\mu\nu}$ is defined as partial derivatives of the $U(1)$ gauge field A_μ as follows,

$$F_{\mu\nu} = \partial_\mu A_\nu - \partial_\nu A_\mu. \quad (2)$$

The tensor $H^{\rho\sigma\delta}$ is the Kalb-Ramond field tensor that is written in terms of the pseudo-scalar axion field ϕ according to,

$$H_{\alpha\beta\delta} = \frac{1}{2} e^{4\xi} \varepsilon_{\alpha\beta\delta\gamma} \partial^\gamma \phi, \quad (3)$$

that responsible to the coupling between the pseudo scalar axion field and the dilaton field. As a result of this, axions become a inherent hair of the rotating black hole instead of becoming a part of the accretion disk.

A. The Metric

The Dyonic Kerr-Sen black hole in Boyer-Lindquist coordinates is described by this following spacetime separation [29, 30],

$$ds^2 = - \left[1 - \frac{r_s(r-d) - r_D^2}{\rho^2} \right] dt^2 + \frac{\rho^2}{\Delta} dr^2 + \rho^2 d\theta^2 - 2 \frac{r_s(r-d) - r_D^2}{\rho^2} a \sin^2 \theta dt d\phi + \sin^2 \theta d\phi^2 \times \left[r(r-2d) - k^2 + a^2 + \frac{r_s(r-d) - r_D^2}{\rho^2} a^2 \sin^2 \theta \right],$$

where,

$$\rho^2 = r(r - 2d) - k^2 + a^2 \cos^2 \theta, \quad (4)$$

$$\Delta = r(r - 2d) - r_s(r - d) - k^2 + a^2 + r_D^2, \quad (5)$$

where the new variables in above equations are related to the physical properties by,

$$r_D^2 = Q^2 + P^2, \quad (6)$$

$$k = \frac{2PQ}{r_s}, \quad (7)$$

$$d = \frac{P^2 - Q^2}{r_s}, \quad (8)$$

$$a = \frac{J}{Meq}, \quad (9)$$

where the parameters of the black hole are mass M , angular momentum per unit mass $a = \frac{J}{M}$, electric charge Q , magnetic charge P , dilaton charge d , and axion charge k .

The condition $\Delta = 0$ makes the g_{rr} divergent, indicating one way surfaces, i.e., the black hole's horizons. The horizons' positions are then obtained by solving this following quadratic equation,

$$\Delta = 0 = r(r - 2d) - r_s(r - d) - k^2 + a^2 + r_D^2, \quad (10)$$

$$r_{\pm} = \frac{r_s}{2} + d \pm \sqrt{\left(\frac{r_s}{2}\right)^2 + d^2 + k^2 - (a^2 + r_D^2)}, \quad (11)$$

where r_+ and r_- are the outer and inner horizons, respectively. Thus, it is possible to rewrite the Δ as,

$$\Delta = (r - r_+)(r - r_-). \quad (12)$$

Remarkably, there are double ellipsoidal singularities at $\rho^2 = 0$ or $r = r_{p,m}$ where

$$r_{p,m} = d \pm \sqrt{d^2 + k^2 - a^2 \cos^2 \theta}, \quad (13)$$

respectively. These are also the zeroes of g_{rr} .

One can also derive the metric determinant $g = \det(g_{\mu\nu})$ and the metric inverse $g^{\mu\nu}$. After some straightforward algebras we find,

$$g = -\rho^4 \sin^2 \theta, \quad (14)$$

and,

$$g^{\mu\nu} = \begin{pmatrix} -\frac{f^{\phi\phi}}{\Delta} & 0 & 0 & \frac{g_{0\phi}}{\Delta \sin^2 \theta} \\ 0 & \frac{\Delta}{\rho^2} & 0 & 0 \\ 0 & 0 & \frac{1}{\rho^2} & 0 \\ \frac{g_{0\phi}}{\Delta \sin^2 \theta} & 0 & 0 & \frac{1}{\Delta \sin^2 \theta} \left(1 - \frac{r_s(r-d) - r_D^2}{\rho^2}\right) \end{pmatrix}, \quad (15)$$

$$f^{\phi\phi} = r(r - 2d) - k^2 + a^2 + \frac{r_s(r - d) - r_D^2}{\rho^2} a^2 \sin^2 \theta. \quad (16)$$

III. THE CLOSED TIMELIKE CURVES

Closed Timelike Curve (CTC) is a closed 1-dimensional curve in 4-dimensional spacetime where each tangent vector to the curve at every point is timelike. CTC has been found in a certain region of some well-known spacetime such as Tipler rotating cylinder [31], Gödel universe [32], Gott's time machine [33], Wheeler worm-holes [34], Alcubierre's warp drive spacetimes [35], rotating cosmic string [36], axially symmetric spacetime with pure radiation [37] and locally AdS [38], Kerr and Kerr-Newman black hole (KNBH) [39], several analog gravity systems [40] and in various modified gravity scenarios [41–44]. In the case of subextremal rotating black holes, the CTC is found inside the inner horizon of the Kerr spacetime while for the case of the electrically charged Kerr-Newman black hole, the CTCs exist both in the region inside the inner horizon and between its two horizons [45]. In this section, we will investigate in which region do CTCs exist in the Dyonic Kerr-Sen spacetime.

Let us consider the basis vector ∂_ϕ . Since the ϕ is periodic, if the basis vector ∂_ϕ is timelike for any constant $t = t_0, r = r_0$ and $\theta = \theta_0$, then a circle (1-sphere) specified by a set of points $\{x \mid t = t_0, r = r_0, \theta = \theta_0\}$ describes a CTC. The region where CTCs exist can be found by investigating the metric component $g_{\phi\phi}$, i.e., whenever $g_{\phi\phi} < 0$, the basis vector ∂_ϕ will be timelike and that indicates the existence of CTCs.

The $g_{\phi\phi}$ component has the form of fourth degree polynomials in the numerator, but it also contains a point of constant radius at $\rho^2 = 0$ in the denominator where the function discontinued between positive infinity and negative infinity, the singularities. Further inspection shows that there are at most 6 CTC boundaries, characterized by four roots r_1, r_2, r_3, r_4 of the numerator of $g_{\phi\phi} = 0$, and two radii r_p, r_m of the singularities.

In the equatorial plane $\theta = \pi/2$, one of the roots ($r_1 - r_4$) is simply r_p and cancelled with the zero of $\rho^2 = 0$ in the denominator. This implies that there are at most 4 boundaries, three (r_1, r_2, r_3) are roots of $g_{\phi\phi} = 0$ and one (r_m) is a singularity. Their expressions are given in Eqn. (17)-(20).

$$r_1 = \frac{1}{3r_s^3} \left[2(P^2 - 2Q^2)r_s^2 + \frac{X_1}{X_2^{1/3}} + X_2^{1/3} \right], \quad (17)$$

$$r_2 = \frac{1}{3r_s^3} \left[2(P^2 - 2Q^2)r_s^2 + \frac{(-1 + i\sqrt{3})}{2} \frac{X_1}{X_2^{1/3}} - \frac{(1 + i\sqrt{3})}{2} X_2^{1/3} \right], \quad (18)$$

$$r_3 = \frac{1}{3r_s^3} \left[2(P^2 - 2Q^2)r_s^2 - \frac{(1 + i\sqrt{3})}{2} \frac{X_1}{X_2^{1/3}} + \frac{(-1 + i\sqrt{3})}{2} X_2^{1/3} \right], \quad (19)$$

$$r_m = -\frac{2Q^2}{r_s}, \quad (20)$$

$$X_1 = r_s^4 \left[4(P^2 + Q^2)^2 - 3a^2 r_s^2 \right], \quad (21)$$

$$X_2 = 8(P^2 + Q^2)^3 r_s^6 - 9(P^2 + Q^2)a^2 r_s^8 - \frac{27}{2} a^2 r_s^{10} + X_3, \quad (22)$$

$$X_3 = \frac{3\sqrt{3}}{2} r_s^8 \sqrt{a^2 \left[4(a^2 + 9(P^2 + Q^2))a^2 r_s^2 - 4(P^2 + Q^2)^2(a^2 + 8(P^2 + Q^2)) + 27a^2 r_s^4 \right]} \quad (23)$$

In Fig. 1-4, the contour plots of the four boundaries r_1, r_2, r_3, r_m are shown. The plots exhibit the numerical values of the boundaries at each set of parameters a, P, Q where the mass parameter is fixed at $r_s = 2$. The white regions in the plots indicate the solution is complex and there will be no physical CTC boundary at those parameters' values. From the three roots $r_1 - r_3$, there is always only one real root for small-charge cases and all three of them are real in large-charge case. On the other hands, r_m is always real. This is why the boundaries of the CTC in Dyonic Kerr-Sen BH (KSBH) appears in pair in equatorial plane, hence created a bounded region(s) of CTC and there will be no CTC at either positive or negative infinity of radial coordinate. It must be noted here that the index of the solutions does not indicate the radial order of them. For example, at low electric charges and magnetic charges, r_1 is the innermost boundary, where at higher charges it becomes the outermost boundary.

In Fig. 5-6, the contour plot of the two horizons are shown in the same manner to the four boundaries. The white region again shows the set of parameters where the roots are complex and there is no horizons, i.e., the superextremal case. The two horizons have the same extremal limit as can be seen from the term in the square root of Eqn. (11). Compare to Kerr-Newman BH, the Dyonic Kerr-Sen BH has an interesting unique property lacking in Kerr-Newman. Consider initially a Dyonic Kerr-Sen BH with no electric and magnetic charge ($P, Q = 0$), but having small enough value of angular momentum to be a subextremal BH. Continuously increasing the charges will result in the BH crossing the extremal limit and becomes superextremal. This is presented by the white region in Fig. 5,6 where both horizons vanish. However, if we continue to increase the charges, the BH will again cross the extremal limit and return to subextremal, in contrast to the KNBH where further increase of charges only results in superextremal spacetime

or naked singularity.

Another property of KSBH is that both the horizons can have negative value of r , this is shown in Fig. 5,6 in the 'blue' region where the electric charge is large and the magnetic charge is small. This signifies the BH can have naked singularities even when it is subextremal, this is further discussed in the following parts.

A. Small and Large charge KSBH: Naked singularity solution

To obtain full structure of the spacetime including the singularities, CTC regions and the two horizons, we plot the metric function g_{rr} and $g_{\phi\phi}$ versus the radial distance r for certain choice of parameters in Fig. 7-10. The singularities $r_{p,m}$ are at $g_{rr} = 0$. The CTC boundary listed in each figure is the outermost boundary. We found that in the very small-charge case, there are two CTC boundaries corresponding to r_1 and r_m pair (see Fig. 1-4). For slightly larger charges (small-charge case), there are two CTC boundaries from r_3 and r_m . In any cases, r_m is always the outer boundary as shown in Fig. 7 and Fig. 8. The two cases are similar to the KNBH where all the CTCs are hidden behind the horizons, but for the moderate-charge and large-charge case, this statement no longer holds. For these cases (Fig. 10), all 4 boundaries exist.

Both moderate-charge and large-charge spacetimes have naked singularity in the large r region. In the large-charge case, the outermost CTC boundary goes beyond the outer horizon r_+ , showing there exists a small CTC 'island' outside of the horizons. However, this occurs in the region of spacetime where g_{rr} is negative, indicating that the ∂_r vector is also timelike, hence this 'island' spacetime is unphysical. This behaviors only occur in the large-charge case because the outermost surface of

constant radius where g_{rr} changes signs from positive to negative lies outside the outer horizon, as oppose to the smaller charge case where they coincides. For the moderate charge case (which we set the same condition as the superextremal case) where there is no horizons, generically there could be either 2 or 4 CTC boundaries as can be seen from the contour plots.

The large-charge KSBH such as depicted in Fig. 10 behaves like an exotic antigravity spacetime in the large $r > r_p$ region with the presence of naked singularity at r_p . The metric function indicates gravity becomes *repulsive* in this region and it is infinitely repulsive at the singularity, i.e., nothing can reach the naked singularity from this side of spacetime. Interestingly, behind the horizon at $r_+ < r_p$, there is a physical spacetime region $r_- < r < r_+$ which allows the existence of CTCs. However, observer in this region will see a cosmic horizon at r_+ and will never be in (classical) contact with the region $r > r_p$.

One may do further analytical investigation on conditions of the the Dyonic Kerr-Sen black hole's parameters and their relations to the $g_{rr}, g_{\phi\phi}$ to check whether CTC could be found in the physical spacetime outside the event horizon, r_+ . First of all, using (6)-(8), we can write r_{\pm} and $\delta_r = r_+ - r_-$ explicitly in the terms of black hole's parameters, r_s, a, Q, P , as follows,

$$r_{\pm} = \frac{r_s}{2} + \frac{P^2 - Q^2}{r_s} \pm \frac{1}{2}\delta_r, \quad (24)$$

$$\delta_r = \sqrt{\frac{(r_s^2 - 2(P^2 + Q^2))^2}{r_s^2} - 4a^2}. \quad (25)$$

Since we are interested in the case of subextremal black hole, it is clear that δ_r must be larger than zero. This condition leads to two possibilities as follows,

$$1. \quad P^2 + Q^2 - \frac{r_s^2}{2} < -r_s\sqrt{a^2}, \quad (26)$$

$$2. \quad P^2 + Q^2 - \frac{r_s^2}{2} > r_s\sqrt{a^2}, \quad (27)$$

where the case (1.) leads to a lightly charged black hole, where the electric charge must follow the inequality, $0 < Q^2 < \frac{r_s^2}{2} - P^2 - r_s\sqrt{a^2}$, and the case (2.) leads to a highly charge black hole, where the electric charge must follow the inequality, $Q^2 > \frac{r_s^2}{2} - P^2 + r_s\sqrt{a^2}$. The case (2.) is the special feature of the Dyonic Kerr-Sen black hole where high (Q)-charge black hole solution is possible without a naked singularity. This is the 'blue' region mentioned earlier in Fig. 1-4.

Let us consider the singularities at $\theta = \pi/2$,

$$r_p = \frac{2P^2}{r_s}, \quad (28)$$

$$r_m = -\frac{2Q^2}{r_s}, \quad (29)$$

where it is clear that for general non zero $P^2 > 0$ and $Q^2 > 0$, r_p will be positive and r_m will be negative.

One can show that the condition $r_p > r_+$ leads to $a^2 > 0$ as follows,

$$\frac{2P^2}{r_s} > \frac{r_s}{2} + \frac{P^2 - Q^2}{r_s} + \frac{\delta_r}{2}, \quad (30)$$

substituting δ_r by (25), clearly the condition is $a^2 > 0$. However, either the condition (26) or (27) also needs to be satisfied. One can rearrange (30) so that,

$$P^2 + Q^2 - \frac{r_s^2}{2} > \frac{1}{2}r_s\delta_r > 0, \quad (31)$$

which implies that $r_p > r_+$ happens only when (27) is valid. So the black hole must be rotating and highly charged. Similarly, one can also check the condition for $r_m < r_-$ and find exactly the same condition as for $r_p > r_+$. Therefore, for large-charge Dyonic Kerr-Sen black hole, the following ordering holds,

$$r_m < r_- < r_+ < r_p. \quad (32)$$

For small-charge Dyonic Kerr-Sen black hole, one may follow the same procedure and find that $r_p < r_-$ leads to the condition $a^2 > 0$ and (26). Therefore the following ordering holds,

$$r_m < r_p < r_- < r_+, \quad (33)$$

for the small-charge KSBH. There is no possible black hole solution with r_p between r_- and r_+ .

Now, let us consider $g_{\phi\phi}$ at $\theta = \pi/2$. After some rearrangement, one can express $g_{\phi\phi}$ as follows,

$$g_{\phi\phi} = \frac{1}{\rho^2} [(\rho^2 + a^2)^2 - a^2\Delta], \quad (34)$$

$$\rho^2 = \left(r - 2\frac{P^2}{r_s}\right) \left(r + 2\frac{Q^2}{r_s}\right), \quad (35)$$

or, in the terms of r_m, r_p at $\theta = \pi/2$, we obtain,

$$\rho^2 = (r - r_p)(r - r_m), \quad (36)$$

At the black hole's horizons, $\Delta = 0$ and $g_{\phi\phi}$ is simplified as follows,

$$g_{\phi\phi}(r_{\pm}) = \frac{(\rho^2 + a^2)^2}{(r_{\pm} - r_p)(r_{\pm} - r_m)}, \quad (37)$$

after some lines of straightforward algebras, one finds,

$$g_{\phi\phi}(r_+) = -r_s^2 \frac{P^2 + Q^2 - \frac{r_s^2}{2} - \frac{r_s}{2}\delta_r}{P^2 + Q^2 + \frac{r_s^2}{2} + \frac{r_s}{2}\delta_r}, \quad (38)$$

$$g_{\phi\phi}(r_-) = -r_s^2 \frac{P^2 + Q^2 - \frac{r_s^2}{2} + \frac{r_s}{2}\delta_r}{P^2 + Q^2 + \frac{r_s^2}{2} - \frac{r_s}{2}\delta_r}. \quad (39)$$

The condition $g_{\phi\phi}(r_+) < 0$ implies that

$$P^2 + Q^2 > \frac{r_s^2}{2} + \frac{r_s}{2}\delta_r, \quad (40)$$

which leads to the simple condition $a^2 > 0$. However, using (26) and (27), we can conclude that (40) can only be true for (27), i.e., the large-charge BH. CTC can exist in the region $r \geq r_+$ if the black hole's angular momentum, a , has value in such a way that,

$$0 < a^2 < \frac{1}{4r_s^2} [2(Q^2 + P^2) - r_s^2]^2. \quad (41)$$

Now, let us investigate the behavior of $g_{\phi\phi}$ in the region $r > r_+$. The function $g_{\phi\phi}$ can be written in its most simplified form as follows,

$$g_{\phi\phi} = \frac{1}{r_s^2 (rr_s + 2Q^2)} F_\phi, \quad (42)$$

where,

$$F_\phi = r_s [4Q^4 r + 2Q^2 r_s (2r^2 + a^2) + r^2 \{r^3 + a^2(a + r_s)\}] - 2P^2 (rr_s + 2Q^2)^2. \quad (43)$$

Since the $g_{\phi\phi}$ in (42) can be thought as a multiplication of two functions, where the first term is clearly always positive in the region $r > r_m = -\frac{2Q^2}{r_s}$, we need further searching for extrema of F_ϕ by finding the root of $\partial_r F_\phi = 0$. The resulting equation is a quartic equation that only has two distinct roots as follows,

$$r_{\phi\pm} = \frac{1}{3} \left[\frac{2P^2 - 4Q^2}{r_s} \pm \sqrt{\frac{4(P^2 + Q^2)^2}{r_s^2} - 3a^2} \right]. \quad (44)$$

From this, we can estimate the general shape of F_ϕ from $r \rightarrow -\infty$ to $r \rightarrow \infty$ as follows: it comes from $-\infty$, increases until reaches its local maxima at $r_{\phi-}$, then decrease reaches its local minima at $r_{\phi+}$, then monotonically increases heading to $+\infty$. One can verify that the local minima is always located inside the black hole's outer horizon, $r_+ > r_{\phi+}$ as follows,

$$r_+ - r_{\phi+} = \frac{1}{6} \left[\frac{2(P^2 + Q^2)}{r_s} + 3(r_s + \delta_r) - 2\sqrt{\frac{4(P^2 + Q^2)^2}{r_s^2} - 3a^2} \right] > 0. \quad (45)$$

Therefore, for small-charge BH (26), $g_{\phi\phi}(r_+) > 0$ and since $g_{\phi\phi}$ is monotonically increasing in the region $r > r_+$, it is impossible to find CTC in the region $r > r_+$.

Now we consider the region around the inner horizon, $r = r_-$. For $r_s > \delta_r$ (small charge) KSBH, since $a^2 > 0$ implies that

$$P^2 + Q^2 < \frac{r_s^2}{2} - \frac{r_s}{2} \delta_r, \quad (46)$$

$g_{\phi\phi}(r_-)$ is always positive and there is no CTC.

On the other hand for $r_s < \delta_r$ (large charge) KSBH, since $a^2 > 0$ implies that the numerator of (39) is always positive and the denominator is always negative, $g_{\phi\phi}(r_-)$ is always negative and there are CTCs around $r = r_-$ region.

Examining $\partial_r g_{\phi\phi}$, we reveal that there is an asymptote at $r_m = -\frac{2Q^2}{r_s}$, the inner singularity. The behavior of $g_{\phi\phi}$ around the asymptote can be investigated as follows. First, let us make a Taylor series around $r = r_m$ as follows,

$$g_{\phi\phi} \approx a^2 \left[\frac{r_s}{r - r_m} + 1 \right], \quad (47)$$

and this shows that approaching $r = r_m$ from the right, $g_{\phi\phi} \rightarrow +\infty$, and approaching from the left, $g_{\phi\phi} \rightarrow -\infty$. The fact that approaching from the left, $g_{\phi\phi} \rightarrow -\infty$, this indicates there will always be region with CTC on the left side of $r = r_m$, which is always inside r_- .

For highly charged black hole, since $r_p > r_+$, we need to check the signature of $g_{\phi\phi}$ at r_p to see whether CTC can exist in the physical exterior space. We obtain,

$$g_{\phi\phi}(r_p) = \frac{2a^2}{a(P^2 + Q^2)} \left[P^2 + Q^2 + \frac{r_s^2}{2} \right] > 0. \quad (48)$$

Since $g_{\phi\phi}$ is monotonically increasing in the region $r \geq r_p$, there is no CTC in the physical exterior space.

IV. THE KLEIN-GORDON EQUATION

The Klein-Gordon equation is a covariant relativistic wave equation that describes the dynamics of a massive or massless spin-0 particle in a particular spacetime. The equation reads as follows,

$$\left[\nabla_\mu \nabla^\mu - \left(\frac{mc}{\hbar} \right)^2 \right] \psi = 0, \quad (49)$$

where ∇_μ is the covariant derivative, m the rest mass of the scalar field ψ . As the covariant derivatives act to a scalar field ψ , they can be rewritten explicitly as the Laplace-Beltrami operator as follows,

$$\left[\frac{1}{\sqrt{-g}} \partial_\mu (\sqrt{-g} g^{\mu\nu} \partial_\nu) - \left(\frac{mc}{\hbar} \right)^2 \right] \psi = 0. \quad (50)$$

Note that the differential operator acts first to the field ψ in the right-to-left order, $\partial(A\partial)\psi = \partial(A\partial\psi)$.

Using the metric inverse (15), we thoroughly construct the explicit form of each component of the Laplace-Beltrami operator in the Dyonic Kerr-Sen black hole as follows,

$$\frac{1}{\sqrt{-g}}\partial_0(\sqrt{-g}g^{00}\partial_0)=-\frac{1}{\Delta\rho^2}\left\{[r(r-2d)-k^2+a^2]^2-\Delta a^2\sin^2\theta\right\}\partial_{ct}^2, \quad (51)$$

$$\frac{1}{\sqrt{-g}}\partial_0(\sqrt{-g}g^{03}\partial_3)=-\frac{[r(r-2d)-k^2+a^2-\Delta]a}{\Delta\rho^2}\partial_{ct}\partial_\phi, \quad (52)$$

$$\frac{1}{\sqrt{-g}}\partial_3(\sqrt{-g}g^{30}\partial_0)=-\frac{[r(r-2d)-k^2+a^2-\Delta]a}{\Delta\rho^2}\partial_{ct}\partial_\phi, \quad (53)$$

$$\frac{1}{\sqrt{-g}}\partial_1(\sqrt{-g}g^{11}\partial_1)=\frac{1}{\rho^2}\partial_r(\Delta\partial_r), \quad (54)$$

$$\frac{1}{\sqrt{-g}}\partial_2(\sqrt{-g}g^{22}\partial_2)=\frac{1}{\rho^2\sin\theta}\partial_\theta(\sin\theta\partial_\theta), \quad (55)$$

$$\frac{1}{\sqrt{-g}}\partial_3(\sqrt{-g}g^{33}\partial_3)=\frac{\Delta-a^2\sin^2\theta}{\Delta\sin^2\theta\rho^2}\partial_\theta^2, \quad (56)$$

$$(57)$$

and after collecting all of the terms, we obtain this following differential equation,

$$\begin{aligned} & \left[-\frac{1}{\Delta\rho^2}\left\{[r(r-2d)-k^2+a^2]^2-\Delta a^2\sin^2\theta\right\}\partial_{ct}^2 \right. \\ & \quad -2\frac{[r(r-2d)-k^2+a^2-\Delta]a}{\Delta\rho^2}\partial_{ct}\partial_\phi \\ & \quad +\frac{1}{\rho^2}\partial_r(\Delta\partial_r)+\frac{1}{\rho^2\sin\theta}\partial_\theta(\sin\theta\partial_\theta) \\ & \quad \left. +\frac{\Delta-a^2\sin^2\theta}{\Delta\sin^2\theta\rho^2}\partial_\phi^2\right]\psi-\frac{m^2c^2}{\hbar^2}\psi=0. \quad (58) \end{aligned}$$

A. Separation of Variables

Due to the temporal and azimuthal symmetry, this following separation ansatz is applied [47],

$$\psi(t,r,\theta,\phi)=e^{-i\frac{E}{\hbar}ct+im_\ell\phi}R(r)T(\theta). \quad (59)$$

For the sake of notation simplicity, we define these following dimensionless variables, $\Omega=\frac{Er_s}{\hbar c}$ and $\Omega_0=\frac{E_0r_s}{\hbar c}$, as energy parameters. Now, multiplying the whole equation by $\rho^2r^2/\psi(t,r,\theta,\phi)$, we arrive at this following equation,

$$\begin{aligned} & \left[\frac{1}{T\sin\theta}\partial_\theta(\sin\theta\partial_\theta T)-\frac{m_\ell^2}{\sin^2\theta} \right. \\ & \quad \left. -\left(\frac{\Omega_0^2a^2}{r_s^2}-\frac{\Omega^2a^2}{r_s^2}\right)\cos^2\theta\right]+\left[\frac{1}{R}\partial_r(\Delta\partial_r R) \right. \\ & \quad +\frac{\Omega^2}{r_s^2}\frac{(r(r-2d)-k^2+a^2)^2}{\Delta}-\frac{\Omega^2a^2}{r_s^2} \\ & \quad \left. -2\frac{(r(r-2d)-k^2+a^2-\Delta)a}{\Delta}\left(\frac{\Omega m_\ell}{r_s}\right) \right. \\ & \quad \left. +\frac{m_\ell^2a^2}{\Delta}-\frac{\Omega_0^2}{r_s^2}(r(r-2d)-k^2)\right]=0. \quad (60) \end{aligned}$$

Notice that since the terms inside the first squared bracket depends only on θ while the rest are functions of r , they can be separated as follows,

$$\begin{aligned} & \frac{1}{T\sin\theta}\partial_\theta(\sin\theta\partial_\theta T)-\frac{m_\ell^2}{\sin^2\theta} \\ & \quad -\left(\frac{\Omega_0^2a^2}{r_s^2}-\frac{\Omega^2a^2}{r_s^2}\right)\cos^2\theta=-\lambda_\ell^{m_\ell}, \quad (61) \end{aligned}$$

where $\lambda_\ell^{m_\ell}$ is a constant. For static spherically symmetric spacetime of non-rotating black holes, the separation constant $\lambda_\ell^{m_\ell}$ is exactly equal to $\ell(\ell+1)$. Therefore, the polar differential equation has exact solution in terms of the associated Legendre polynomial, $P_\ell^{m_\ell}(\cos\theta)$.

With the presence of black hole's angular momentum, $a\neq 0$, the polar equation is generalized and has series solution named Spheroidal Harmonics, $S_l^{m_\ell}$. The Spheroidal Harmonics can be written as a series expansion of associated Legendre polynomial as its orthonormal basis, given as follows,

$$T(\theta)=S_l^{m_\ell}(\sigma,\cos\theta)=\sum_{r=-\infty}^{\infty}d_r^{lm_\ell}(\sigma)P_{l+r}^{m_\ell}(\cos\theta), \quad (62)$$

where,

$$\sigma=\frac{\Omega_0^2a^2}{r_s^2}-\frac{\Omega^2a^2}{r_s^2}. \quad (63)$$

The coefficient $d_r^{lm_\ell}$ is amplitude of the mode $(l+r), m_\ell$. It is possible, for the case $\sigma < 1$ to algebraically calculate $\lambda_\ell^{m_\ell}$ via perturbation theory [48–52], resulted in this following expression,

$$\lambda_\ell^{m_\ell}=l(l+1)-2\sigma\left(\frac{m_\ell^2+l(l+1)-1}{(2l-1)(2l+3)}\right)+O(\sigma^2). \quad (64)$$

B. The Radial Equation

Having done with the polar equation, we are left with the radial equation as follows,

$$\begin{aligned} \partial_r^2 R + \left(\frac{1}{r-r_-} + \frac{1}{r-r_+} \right) \partial_r R \\ + \frac{1}{\delta_r^2} \left[\left(\frac{1}{r-r_+} - \frac{1}{r-r_-} \right)^2 \times \right. \\ \left. \left\{ \frac{(a^2 - k^2 + r(r-2d) - am_\ell)\Omega}{r_s} \right\}^2 \right. \\ \left. - \delta_r \left(\frac{1}{r-r_+} - \frac{1}{r-r_-} \right) \times \right. \\ \left. \left\{ K_l^{m_\ell} + \frac{(a^2 - k^2 + r(r-2d))\Omega_0^2}{r_s^2} \right\} \right] R = 0, \quad (65) \end{aligned}$$

where the constant $K_l^{m_\ell}$ is used to abbreviate this following expression,

$$K_l^{m_\ell} = \frac{\Omega^2}{r_s^2} a^2 - \frac{\Omega_0^2}{r_s^2} a^2 - 2 \frac{\Omega m_\ell}{r_s} a + \lambda_\ell^{m_\ell}. \quad (66)$$

Now, transforming the radial variable $r \rightarrow x = \frac{(r-r_-)}{\delta_r}$, we obtain radial equation in the terms of x as follows,

$$\partial_r^2 R + \frac{(2x-1)}{(x-1)x} \partial_r R + \frac{T_1^2 + T_2}{\delta_r^2 r_s^2 (x-1)^2 x^2} R = 0, \quad (67)$$

where we have defined,

$$\begin{aligned} T_1 = \frac{1}{\delta_r r_s (x-1)x} [amr_s \\ - \{a^2 - k^2 + (r_- + \delta_r x)(r_- - 2d + \delta_r x)\} \Omega], \quad (68) \end{aligned}$$

and,

$$\begin{aligned} T_2 = -\frac{1}{r_s^2 (x-1)x} [K_\ell^{m_\ell} r_s^2 \\ + \{a^2 - k^2 + (r_- + \delta_r x)(r_- - 2d + \delta_r x)\} \Omega_0^2]. \quad (69) \end{aligned}$$

By applying fractional decomposition to T_1 , we obtain,

$$\begin{aligned} T_1 = -\frac{K_1}{\delta_r x} + \frac{\delta_r \Omega}{r_s} \\ - \frac{-K_1 r_s + (r_-^2 - 2dr_- - r_+^2 + 2dr_+) \Omega}{\delta_r r_s (x-1)}, \quad (70) \end{aligned}$$

where we have defined,

$$K_1 = -\frac{amr_s + (k^2 - a^2 + 2dr_- - r_-^2)\Omega}{r_s}. \quad (71)$$

Let us defined as K_3 as the coefficient of $(x-1)^{-1}$ as follows,

$$K_3 = -\frac{-K_1 r_s + (r_-^2 - 2dr_- - r_+^2 + 2dr_+) \Omega}{\delta_r r_s}, \quad (72)$$

and after some lines of algebras, we can write T_1^2 as follows,

$$\begin{aligned} T_1^2 = \frac{K_3^2}{(x-1)^2} + \frac{K_1^2}{\delta_r^2 x^2} + \frac{\delta_r^2 \Omega^2}{r_s^2} \\ + \frac{2K_1(K_3 r_s - \delta_r \Omega)}{\delta_r r_s x} - \frac{2K_3(K_1 r_s - \delta_r^2 \Omega)}{\delta_r r_s (x-1)}. \quad (73) \end{aligned}$$

Now let us consider T_2 , applying the fractional decomposition, we obtain,

$$\begin{aligned} T_2 = \frac{K_2}{x} - \frac{\delta_r^2 \Omega_0^2}{r_s^2} \\ + \frac{-K_2 r_s^2 + (r_-^2 - 2dr_- - r_+^2 + 2dr_+) \Omega_0^2}{r_s^2 (x-1)}, \quad (74) \end{aligned}$$

where we have defined,

$$K_2 = -\frac{-K_l^{m_\ell} r_s^2 + (k^2 - a^2 + 2dr_- - r_-^2) \Omega_0^2}{r_s^2}, \quad (75)$$

and for the sake of simplicity, let us define K_4 as the coefficient of $(x-1)^{-1}$ as follows,

$$K_4 = \frac{-K_2 r_s^2 + (r_-^2 - 2dr_- - r_+^2 + 2dr_+) \Omega_0^2}{r_s^2}. \quad (76)$$

So, we have simplified T_2 as follows,

$$T_2 = \frac{K_4}{x-1} + \frac{K_2}{x} - \frac{\delta_r^2 \Omega_0^2}{r_s^2}. \quad (77)$$

And the simplified radial equation reads as follows,

$$\begin{aligned} \partial_r^2 R + \left(\frac{1}{x-1} + \frac{1}{x} \right) \partial_r R + \left[\frac{\delta_r^2 (\Omega^2 - \Omega_0^2)}{r_s^2} \right. \\ \left. + \frac{1}{x} \left(K_2 + \frac{2K_1 K_3}{\delta_r} - \frac{2K_1 \Omega}{r_s} \right) + \frac{1}{x^2} \left(\frac{K_1^2}{\delta_r^2} \right) + \right. \\ \left. \frac{1}{x-1} \left(K_4 - \frac{2K_1 K_3}{\delta_r} - \frac{2K_3 \delta_r \Omega}{r_s} \right) + \frac{K_3^2}{(x-1)^2} \right] R = 0 \quad (78) \end{aligned}$$

Comparing with the the Confluent Heun equation in equation (A11), we obtain exact expressions of the confluent Heun's parameters, i.e., $\alpha, \beta, \gamma, \delta$ and η as follows,

$$\alpha_\pm = \pm 2i \frac{\delta_r}{r_s} \sqrt{\Omega^2 - \Omega_0^2}, \quad (79)$$

$$\beta_\pm = \pm \frac{2i}{\delta_r} \left[\frac{\Omega}{r_s} (r_- (r_- - 2d) - k^2 + a^2) - m_\ell a \right], \quad (80)$$

$$\gamma_\pm = \pm \frac{2i}{\delta_r} \left[\frac{\Omega}{r_s} (r_+ (r_+ - 2d) - k^2 + a^2) - m_\ell a \right], \quad (81)$$

$$\delta = \frac{\delta_r}{r_s^2} (r_+ + r_- - 2d) (2\Omega^2 - \Omega_0^2), \quad (82)$$

$$\begin{aligned} \eta = & -\frac{1}{r_s^2} [2\Omega \{-am_\ell r_s + (a^2 - k^2 + r_-(r_- - 2d))\Omega\} \\ & - \frac{2}{\delta_r^2} \{-am_\ell r_s + a^2\Omega - k^2\Omega + r_-(r_- - 2d)\Omega\} \times \\ & \{ -am_\ell r_s + a^2\Omega - k^2\Omega + r_+(r_+ - 2d)\Omega\} \\ & + \{a^2 - k^2 + r_-(r_- - 2d)\}\Omega_0^2 + K_l^{m_\ell} r_s^2]. \end{aligned} \quad (83)$$

Finally, the full exact solution of the radial Klein-Gordon equation in the region inside the Dyonic Kerr-Sen black hole's inner horizon reads as follows,

$$\begin{aligned} R(r) = & e^{\frac{1}{2}\alpha\left(\frac{r-r_-}{\delta_r}\right)} \left(\frac{r-r_+}{\delta_r}\right)^{\frac{1}{2}\gamma} \times \\ & \left[A \left(\frac{r-r_-}{\delta_r}\right)^{\frac{1}{2}\beta} \text{HeunC}\left(\alpha, \beta, \gamma, \delta, \eta, \frac{r-r_-}{\delta_r}\right) \right. \\ & \left. + B \left(\frac{r-r_-}{\delta_r}\right)^{-\frac{1}{2}\beta} \text{HeunC}\left(\alpha, -\beta, \gamma, \delta, \eta, \frac{r-r_-}{\delta_r}\right) \right], \end{aligned} \quad (84)$$

and the asymptotic behaviour at $|r| \gg 1$ reads as follows,

$$R(r) = \frac{1}{|r|} \left[A_\infty e^{-\frac{1}{2}\alpha\left(\frac{|r|}{\delta_r}\right)} |r|^{-\frac{\delta}{\alpha}} + B_\infty e^{\frac{1}{2}\alpha\left(\frac{|r|}{\delta_r}\right)} |r|^{\frac{\delta}{\alpha}} \right]. \quad (85)$$

In general, we find this following tabulated characteristic of quasinormal frequencies,

Parameter	$Re(\Omega)$	$Im(\Omega)$	$Re(\alpha)$	$Re\left(\frac{\delta}{\alpha}\right)$	$Im\left(\frac{\delta}{\alpha}\right)$
$\alpha_+, \beta_+, \gamma_+$	+	+	-	-	-
$\alpha_+, \beta_+, \gamma_-$	-	-	-	-	-
$\alpha_+, \beta_-, \gamma_+$	+	+	-	-	-
$\alpha_+, \beta_-, \gamma_-$	-	-	-	-	-
$\alpha_-, \beta_+, \gamma_+$	-	+	-	-	+
$\alpha_-, \beta_+, \gamma_-$	+	-	-	-	+
$\alpha_-, \beta_-, \gamma_+$	-	+	-	-	+
$\alpha_-, \beta_-, \gamma_-$	+	-	-	-	+

TABLE I: Signature of the Dyonic Kerr-Sen black hole's quasinormal frequencies.

Notice that $Re(\alpha)$ is negative for all modes. This makes the first solution blows up and must be eliminated by setting $A_\infty = 0$. By defining this following new variables,

$$\frac{\delta}{\alpha} = \xi_1 + i\xi_2, \quad (86)$$

$$\alpha = \alpha_1 + i\alpha_2, \quad (87)$$

where the subscript 1 denotes the real part and subscript 2 denotes the imaginary part. we can further identify the

behavior of the asymptotic solution as ingoing/outgoing wave as follows,

$$T(t)R(r) \approx \frac{B_\infty}{|r|} e^{\frac{\alpha_1}{2}\frac{|r|}{\delta_r}} e^{-i\left(\frac{\Omega}{r_s}ct - \xi_2 \ln|r|\right)} |r|^{\xi_1}. \quad (88)$$

The solutions are now regular asymptotically.

V. BLACK HOLE'S QUASIRESONANCE

Putting each combination of the solved Confluent Heun's parameters into the polynomial condition in equation (A5), we obtain eight expressions that are functions of the Dyonic Kerr-Sen black hole's parameters, i.e., mass, angular momentum and charges also the scalar fields' rest and relativistic energy connected to the order of the polynomial n_r . The polynomial condition of the radial exact solution, in fact, is not other than the scalar field's exact energy quantization condition, where n_r is understood as the main radial quantum number.

A. Massive Modes

There are 8 massive modes (i.e., $2 \times 2 \times 2$ possible combinations of α_\pm, β_\pm and γ_\pm), where each solution corresponds to a QNM. Substituting (79)-(82) into (A5), we obtain,

1. For mode with $\alpha_+, \beta_+, \gamma_+$,

$$\frac{(2d - r_- - r_+)(2\Omega^2 - \Omega_0^2)}{2r_s\sqrt{\Omega_0^2 - \Omega^2}} + \frac{i}{r_s\delta_r}\mathfrak{D}_\Omega = -n_r. \quad (89)$$

2. For mode with $\alpha_+, \beta_+, \gamma_-$,

$$-\frac{(2d - r_- - r_+)(\Omega_0^2 - 2\Omega^2 - 2\Omega\sqrt{\Omega^2 - \Omega_0^2})}{2r_s\sqrt{\Omega_0^2 - \Omega^2}} = -n_r. \quad (90)$$

3. For mode with $\alpha_+, \beta_-, \gamma_+$,

$$-\frac{(2d - r_- - r_+)(\Omega_0^2 - 2\Omega^2 + 2\Omega\sqrt{\Omega^2 - \Omega_0^2})}{2r_s\sqrt{\Omega_0^2 - \Omega^2}} = -n_r. \quad (91)$$

4. For mode with $\alpha_+, \beta_-, \gamma_-$,

$$\frac{(2d - r_- - r_+)(2\Omega^2 - \Omega_0^2)}{2r_s\sqrt{\Omega_0^2 - \Omega^2}} - \frac{i}{r_s\delta_r}\mathfrak{D}_\Omega = -n_r. \quad (92)$$

5. For mode with $\alpha_-, \beta_+, \gamma_+$,

$$-\frac{(2d - r_- - r_+)(2\Omega^2 - \Omega_0^2)}{2r_s\sqrt{\Omega_0^2 - \Omega^2}} + \frac{i}{r_s\delta_r}\mathfrak{D}_\Omega = -n_r. \quad (93)$$

6. For mode with $\alpha_-, \beta_+, \gamma_-$,

$$\frac{(2d - r_- - r_+)(\Omega_0^2 - 2\Omega^2 + 2\Omega\sqrt{\Omega^2 - \Omega_0^2})}{2r_s\sqrt{\Omega_0^2 - \Omega^2}} = -n_r. \quad (94)$$

7. For mode with $\alpha_-, \beta_-, \gamma_+$,

$$\frac{(2d - r_- - r_+)(\Omega_0^2 - 2\Omega^2 - 2\Omega\sqrt{\Omega^2 - \Omega_0^2})}{2r_s\sqrt{\Omega_0^2 - \Omega^2}} = -n_r. \quad (95)$$

8. For mode with $\alpha_-, \beta_-, \gamma_-$,

$$-\frac{(2d - r_- - r_+)(2\Omega^2 - \Omega_0^2)}{2r_s\sqrt{\Omega_0^2 - \Omega^2}} - \frac{i}{r_s\delta_r}\mathfrak{D}_\Omega = -n_r, \quad (96)$$

where we have defined,

$$\mathfrak{D}_\Omega = -2am_\ell r_s + [2a^2 - 2k^2 + r_-^2 + r_+^2 - 2d(r_- + r_+)]\Omega. \quad (97)$$

Numerical results for certain choice of parameters for the complex scalar quasinormal frequencies are shown in Fig. 11. The modes representing outgoing solutions at $r \rightarrow -\infty$ require $\xi_2 < 0$, i.e., all modes with α_+ . Thus, we further eliminate all modes with α_- . All of the four outgoing modes have the following properties, i.e., either growing (unstable) if having positive real frequency, or decaying if having negative real frequency. This indicates whenever massive scalar fields enter the region with CTC, instability that causes the massive modes to grow over time occurs as a consequence.

B. Massless Modes

Setting $\Omega_0 = 0$, we find another set of eight massless modes as follows,

1. For mode with $\alpha_+, \beta_+, \gamma_+$,

$$\Omega_1 = \frac{[2am_\ell - in_r(r_- - r_+)]r_s}{2[a^2 - k^2 + r_-(r_- - 2d)]}, \quad (98)$$

$$\Omega_2 = \frac{[2am_\ell - in_r(r_- - r_+)]r_s}{2[a^2 - k^2 + r_+(r_+ - 2d)]}. \quad (99)$$

2. For mode with $\alpha_+, \beta_+, \gamma_-$,

$$\Omega = \frac{in_r r_s}{4d - 2(r_- + r_+)}. \quad (100)$$

3. For mode with $\alpha_+, \beta_-, \gamma_+$,

$$\Omega = -\frac{in_r r_s}{4d - 2(r_- + r_+)}. \quad (101)$$

4. For mode with $\alpha_+, \beta_-, \gamma_-$,

$$\Omega_1 = \frac{[2am_\ell + in_r(r_- - r_+)]r_s}{2[a^2 - k^2 + r_-(r_- - 2d)]}, \quad (102)$$

$$\Omega_2 = \frac{[2am_\ell + in_r(r_- - r_+)]r_s}{2[a^2 - k^2 + r_+(r_+ - 2d)]} \quad (103)$$

5. For mode with $\alpha_-, \beta_+, \gamma_+$,

$$\Omega_1 = \frac{[2am_\ell - in_r(r_- - r_+)]r_s}{2[a^2 - k^2 + r_-(r_- - 2d)]}, \quad (104)$$

$$\Omega_2 = \frac{[2am_\ell - in_r(r_- - r_+)]r_s}{2[a^2 - k^2 + r_+(r_+ - 2d)]}. \quad (105)$$

6. For mode with $\alpha_-, \beta_+, \gamma_-$,

$$\Omega = \frac{in_r r_s}{4d - 2(r_- + r_+)}. \quad (106)$$

7. For mode with $\alpha_-, \beta_-, \gamma_+$,

$$\Omega = -\frac{in_r r_s}{4d - 2(r_- + r_+)}. \quad (107)$$

8. For mode with $\alpha_-, \beta_-, \gamma_-$,

$$\Omega_1 = \frac{[2am_\ell + in_r(r_- - r_+)]r_s}{2[a^2 - k^2 + r_-(r_- - 2d)]}, \quad (108)$$

$$\Omega_2 = \frac{[2am_\ell + in_r(r_- - r_+)]r_s}{2[a^2 - k^2 + r_+(r_+ - 2d)]}. \quad (109)$$

C. Growing Quasinormal frequency and CPC

In this section, we will show that all nonzero-energy massless quasinormal modes (QNMs) within $r < r_-$ region are growing modes. With growing modes, the space-time backreaction would become exponentially enhanced and cause instability of the background spacetime region where CTC exist. For the KSBH spacetime, fluctuation of massless field will destroy the spacetime region with the CTC and CPC is thus proven valid.

From all 8 possibilities of massless quasinormal modes in Sect. VB, only the α_+, β_+ modes, Eqn. (98)-(100), satisfy the boundary conditions of the QNMs, namely

$$R(r \rightarrow -\infty) \rightarrow 0, \\ R(r \rightarrow r_-) \sim \left(\frac{r - r_-}{\delta_r}\right)^{+i\sqrt{A_3}} = x^{\beta_+/2}.$$

Moreover, only the QNMs with nonzero real parts are relevant to the stability analysis of the background spacetime, the purely imaginary modes has zero energy and cannot transmit energy nor information. For all α_+, β_+ modes with nonzero real parts, since $r_+ > r_-$ positive imaginary parts of Eqn. (98)-(99) occur when

$$a^2 - k^2 + r_-(r_- - 2d) > 0, \quad (110)$$

which naturally leads to the condition $a^2 > 0$, the BH simply has to be rotating. From real parts of the modes given in Eqn. (98)-(99) which is proportional to $2m_\ell a$, nonzero energy also requires the field to be circling around the BH with nonzero m_ℓ . Thus, the nonzero energy which is the real part of QNMs and the positivity of the imaginary part of QNMs, both require the rotation of BH. Growing modes lead to exponentially growing field that would generate the backreaction to the spacetime in $r < r_-$ region and cause instability of the spacetime. CPC is proven valid for the KSBH where region with CTC is unstable due to the exponentially growing QNMs.

Numerical studies of the massive modes also found that all the outgoing positive-energy modes that can reach faraway region $x \rightarrow -\infty$ have positive imaginary parts and thus are exponentially growing modes as shown in Fig. 11. But analysis of only massless modes is already sufficient to prove validity of CPC in the KSBH spacetime.

VI. CONCLUSIONS AND DISCUSSIONS

In this work, we consider the Dyonic Kerr-Sen black hole's and its spacetime structure. It is found that subextremal Dyonic Kerr-Sen black holes can be grouped into two categories, i.e., small-charge and large-charge black holes, where the latter is not possible in the Kerr-Newman BH. Comprehensive investigation of the possibilities on where the CTC may exist is then carried out and we found that CTC always exists in the region inside the black hole's inner horizon (Cauchy horizon), $r < r_-$, for both categories. In addition, the contour plots of the CTCs boundaries and plots of metric functions for various combinations of the Dyonic Kerr-Sen black hole's parameters are also presented.

A novel investigation of the relativistic quantum scalar field dynamics in the region inside the black hole's inner horizon where CTCs exist is performed. In this work, it is for the first time the CPC is investigated by exactly solve the Klein-Gordon equation in the region inside the black hole's inner horizon. Detail derivations to obtain the exact radial solutions of the governing Klein-Gordon equation and the quantized energy levels for both massive and massless scalar fields are presented.

For massive fields, numerical analyses reveal that modes with $Re(\Omega) > 0$ are growing over time (unstable) and modes with $Re(\Omega) < 0$ are decaying, indicating whenever massive scalar fields propagate in the region with CTC, instability occurs and massive modes will grow exponentially over time as the consequence. For massless fields, instability occurs for QNMs with nonzero $Re(\Omega)$. It is analytically discovered that the condition (110) for the instability to occur is $a^2 > 0$ (and $m_\ell \neq 0$), i.e., the BH simply has to be rotating and the field has to be circling around the BH. The condition, $a^2 > 0$, is also consistent with the condition that allows the CTC to exist (see (40)). The region with CTCs is unstable and CPC is proven valid for the KSBH.

In contrast to the widely used semi-classical WKB approximation, where the approximation breaks down for low momentum, $p = \hbar k \approx 0$, and also the breaking down of the wave function at regions with potential barriers [53, 54], or the continued fraction method, where it is efficient only for finding complex QNMs with a relatively small real part [55] and does not converge for case of purely imaginary frequencies [55, 56]. In this work, the presented exact results do not exhibit such problems and the solutions are correct for the whole region of interest. Moreover, solving the energy from the obtained quartic

and quadratic equations is undoubtedly much more efficient compared to any fully numerical method since the roots are known exactly.

ACKNOWLEDGMENTS

PB is supported in part by National Research Council of Thailand (NRCT) and Chulalongkorn University under Grant N42A660500. DS acknowledges this work is supported by the Second Century Fund (C2F), Chulalongkorn University, Thailand.

Appendix A: The Confluent Heun Equation

The Confluent Heun differential equation is a linear second order ordinary differential equation, generalization of the Hypergeometric differential equation, having this following canonical form [57],

$$\frac{d^2 y_H}{dx^2} + \left(\alpha + \frac{\beta + 1}{x} + \frac{\gamma + 1}{x - 1} \right) \frac{dy_H}{dx} + \left(\frac{\mu}{x} + \frac{\nu}{x - 1} \right) y_H = 0, \quad (\text{A1})$$

where,

$$\mu = \frac{1}{2} (\alpha - \beta - \gamma + \alpha\beta - \beta\gamma) - \eta, \quad (\text{A2})$$

$$\nu = \frac{1}{2} (\alpha + \beta + \gamma + \alpha\gamma + \beta\gamma) + \delta + \eta. \quad (\text{A3})$$

The solutions are given in two independent Confluent Heun functions as follows,

$$y_H = A \text{HeunC}(\alpha, \beta, \gamma, \delta, \eta, x) + B x^{-\beta} \text{HeunC}(\alpha, -\beta, \gamma, \delta, \eta, x). \quad (\text{A4})$$

The Confluent Heun function can be reduced to an n^{th} order polynomial function if the following series termination condition is fulfilled,

$$\frac{\delta}{\alpha} + \frac{\beta + \gamma}{2} = -n_r, \quad n_r \in \mathbb{N}. \quad (\text{A5})$$

Suppose we have a natural general form of the asymmetrical Confluent Heun equation [18, 57],

$$\frac{d^2 y}{dx^2} + \left(\frac{1}{x} + \frac{1}{x - 1} \right) \frac{dy}{dx} + \left(\frac{A_1}{x} + \frac{A_2}{x - 1} + \frac{A_3}{x^2} + \frac{A_4}{(x - 1)^2} + A_5 \right) y = 0, \quad (\text{A6})$$

in order to find the solution of (A6), we have to apply the s-homotopic transformation [18, 57–60] by transforming the dependent variable $y(x) \rightarrow u(x)$ as follows,

$$y(x) = e^{B_0 x} x^{B_1} (x - 1)^{B_2} u(x). \quad (\text{A7})$$

Substituting the transformation into the equation (A6), we find the values of the exponents B_0, B_1, B_2 from the initial equation as follows,

$$B_0(B_0 - 1) + B_0 + A_5 = 0 \rightarrow B_0 = \pm i\sqrt{A_5}, \quad (\text{A8})$$

$$B_1(B_1 - 1) + B_1 + A_3 = 0 \rightarrow B_1 = \pm i\sqrt{A_3}, \quad (\text{A9})$$

$$B_2(B_2 - 1) + B_2 + A_4 = 0 \rightarrow B_2 = \pm i\sqrt{A_4}. \quad (\text{A10})$$

Thus, after obtaining the three exponents, substitution of the s-homotopic transformation (A7) into (A6) leads to a differential equation for $u(x)$ as follows,

$$\frac{d^2u}{dx^2} + \left(2B_0 + \frac{2B_1 + 1}{x} + \frac{2B_2 + 1}{x-1}\right) \frac{du}{dx} + \left(\frac{\sigma}{x} + \frac{\chi}{x-1}\right) u = 0, \quad (\text{A11})$$

where

$$\sigma = -B_1 - B_2 - 2B_1B_2 + B_0 + 2B_0B_1 + A_1, \quad (\text{A12})$$

$$\chi = B_1 + B_2 + 2B_1B_2 + B_0 + 2B_0B_2 + A_2. \quad (\text{A13})$$

By comparing (A11) with (A1), we can write the solution for $u(x)$ in terms of the Confluent Heun functions as follows,

$$u = A \text{HeunC}(\alpha, \beta, \gamma, \delta, \eta, x) + Bx^{-\beta} \text{HeunC}(\alpha, -\beta, \gamma, \delta, \eta, x), \quad (\text{A14})$$

where,

$$\alpha = 2B_0 = \pm 2i\sqrt{A_5}, \quad (\text{A15})$$

$$\beta = 2B_1 = \pm 2i\sqrt{A_3}, \quad (\text{A16})$$

$$\gamma = 2B_2 = \pm 2i\sqrt{A_4}, \quad (\text{A17})$$

$$\delta = A_1 + A_2, \quad (\text{A18})$$

$$\eta = -A_1. \quad (\text{A19})$$

Hence, the complete solutions for the natural general form of the asymmetrical Confluent Heun equation (A6) are obtained as follows,

$$y = e^{\pm i\sqrt{A_5}x} x^{\pm i\sqrt{A_3}} (x-1)^{\pm i\sqrt{A_4}} [A \text{HeunC}(\alpha, \beta, \gamma, \delta, \eta, x) + Bx^{-\beta} \text{HeunC}(\alpha, -\beta, \gamma, \delta, \eta, x)], \quad (\text{A20})$$

with $\alpha, \beta, \gamma, \delta, \eta$ are given by (A.15)-(A.19).

For $x \rightarrow \infty$, the approximate solution of (A1) is given as follows,

$$y_{H\infty} = A_\infty x^{-\left(\frac{\delta}{\alpha} + \frac{\beta + \gamma + 2}{2}\right)} + B_\infty e^{-\alpha x} x^{\left(\frac{\delta}{\alpha} - \frac{\beta + \gamma + 2}{2}\right)} = e^{-\frac{1}{2}\alpha x} x^{-\frac{\beta + \gamma + 2}{2}} \left[A_\infty e^{\frac{1}{2}\alpha x} x^{-\frac{\delta}{\alpha}} + B_\infty e^{-\frac{1}{2}\alpha x} x^{\frac{\delta}{\alpha}} \right], \quad (\text{A21})$$

or, in the form (A20), we get,

$$y = \frac{1}{x} \left[A_\infty e^{\frac{1}{2}\alpha x} x^{-\frac{\delta}{\alpha}} + B_\infty e^{-\frac{1}{2}\alpha x} x^{\frac{\delta}{\alpha}} \right]. \quad (\text{A22})$$

-
- [1] B. P. Abbott *et al.* [LIGO Scientific and Virgo], “Observation of Gravitational Waves from a Binary Black Hole Merger,” *Phys. Rev. Lett.* **116** (2016) no.6, 061102 doi:10.1103/PhysRevLett.116.061102 [arXiv:1602.03837 [gr-qc]].
- [2] J. Drori, Y. Rosenberg, D. Bermudez, Y. Silberberg and U. Leonhardt, “Observation of Stimulated Hawking Radiation in an Optical Analogue,” *Phys. Rev. Lett.* **122** (2019) no.1, 010404 doi:10.1103/PhysRevLett.122.010404 [arXiv:1808.09244 [gr-qc]].
- [3] J. R. Muñoz de Nova, K. Golubkov, V. I. Kolobov and J. Steinhauer, *Nature* **569**, no.7758, 688-691 (2019) doi:10.1038/s41586-019-1241-0 [arXiv:1809.00913 [gr-qc]].
- [4] P. M. Chesler, E. Curiel and R. Narayan, “Numerical evolution of shocks in the interior of Kerr black holes,” *Phys. Rev. D* **99**, no.8, 084033 (2019) doi:10.1103/PhysRevD.99.084033 [arXiv:1808.07502 [gr-qc]].
- [5] N. Zilberman, M. Casals, A. Ori and A. C. Ottewill, “Quantum Fluxes at the Inner Horizon of a Spinning Black Hole,” *Phys. Rev. Lett.* **129**, no.26, 261102 (2022) doi:10.1103/PhysRevLett.129.261102 [arXiv:2203.08502 [gr-qc]].
- [6] T. McMaken, “Backreaction from quantum fluxes at the Kerr inner horizon,” [arXiv:2405.13221 [gr-qc]].
- [7] T. McMaken and A. J. S. Hamilton, “Hawking radiation inside a rotating black hole,” *Phys. Rev. D* **109**, no.6, 065023 (2024) doi:10.1103/PhysRevD.109.065023 [arXiv:2401.03098 [gr-qc]].
- [8] R. Casadio, B. Harms, Y. Leblanc and P. H. Cox, “New perturbative solutions of the Kerr-Newman dilatonic black hole field equations,” *Phys. Rev. D* **55**, 814-825 (1997) doi:10.1103/PhysRevD.55.814 [arXiv:hep-th/9606069 [hep-th]].
- [9] R. R. Hsu and W. F. Lin, “Axionic Kerr black hole,” *Class. Quant. Grav.* **8**, L161-L166 (1991) doi:10.1088/0264-9381/8/8/002
- [10] A. Garcia, D. Galtsov and O. Kechkin, “Class of stationary axisymmetric solutions of the Einstein-Maxwell dilaton - axion field equations,” *Phys. Rev. Lett.* **74**, 1276-1279 (1995) doi:10.1103/PhysRevLett.74.1276
- [11] I. Semiz, *Gen. Rel. Grav.* **43**, 833-846 (2011) doi:10.1007/s10714-010-1108-z [arXiv:gr-qc/0508011 [gr-qc]].
- [12] M. F. A. R. Sakti and P. Burikham, *Phys. Rev. D* **106** (2022) no.10, 106006 doi:10.1103/PhysRevD.106.106006 [arXiv:2206.10868 [hep-th]].
- [13] M. F. A. R. Sakti and P. Burikham, *Eur. Phys. J. C* **84** (2024) no.2, 182 doi:10.1140/epjc/s10052-024-12537-8 [arXiv:2307.04929 [hep-th]].

- [14] S. W. Hawking, “The Chronology protection conjecture,” *Phys. Rev. D* **46**, 603-611 (1992) doi:10.1103/PhysRevD.46.603
- [15] H. a. Shinkai and S. A. Hayward, “Fate of the first traversible wormhole: Black hole collapse or inflationary expansion,” *Phys. Rev. D* **66**, 044005 (2002) doi:10.1103/PhysRevD.66.044005 [arXiv:gr-qc/0205041 [gr-qc]].
- [16] I. D. Novikov and D. I. Novikov, “Collapse of a Wormhole and its Transformation into Black Holes,” *J. Exp. Theor. Phys.* **129**, no.4, 495-502 (2019) doi:10.1134/S1063776119100248
- [17] M. Visser, [arXiv:gr-qc/0204022 [gr-qc]].
- [18] H. S. Vieira, V. B. Bezerra and C. R. Muniz, “Instability of the charged massive scalar field on the Kerr–Newman black hole spacetime,” *Eur. Phys. J. C* **82** (2022) no.10, 932 doi:10.1140/epjc/s10052-022-10908-7 [arXiv:2107.02562 [gr-qc]].
- [19] D. Senjaya, “Exact analytical quasibound states of a scalar particle around a slowly rotating black hole,” *JHEAp* **40** (2023), 49-54 doi:10.1016/j.jheap.2023.10.002
- [20] D. Senjaya, “Exact analytical quasibound states of a scalar particle around a Reissner–Nordström black hole,” *Phys. Lett. B* **848** (2024), 138373 doi:10.1016/j.physletb.2023.138373
- [21] D. Senjaya, “Exact massive and massless scalar quasibound states around a charged Lense–Thirring black hole,” *Phys. Lett. B* **849** (2024), 138414 doi:10.1016/j.physletb.2023.138414
- [22] D. Senjaya, “Exact scalar quasibound states solutions of f(R) theory’s static spherically symmetric black hole,” *JHEAp* **41** (2024), 61-66 doi:10.1016/j.jheap.2024.01.004
- [23] D. Senjaya, “Exact massless scalar quasibound states of the Ernst black hole,” *Eur. Phys. J. C* **84** (2024) no.1, 57 doi:10.1140/epjc/s10052-024-12422-4
- [24] D. Senjaya, “Exact massive and massless scalar quasibound states solutions of the Einstein–Maxwell–dilaton (EMD) black hole,” *Eur. Phys. J. C* **84** (2024) no.3, 229 doi:10.1140/epjc/s10052-024-12600-4
- [25] D. Senjaya, “Exact phonon quasibound states around an optical black hole,” *Eur. Phys. J. C* **84** (2024) no.4, 388 doi:10.1140/epjc/s10052-024-12755-0
- [26] D. Senjaya, P. Burikham and T. Harko, “The Exact Relativistic Scalar Quasibound States of The Dyonic Kerr–Sen Black Hole: Quantized Energy, and Hawking Radiation,” [arXiv:2405.15219 [gr-qc]].
- [27] A. Sen, “Rotating charged black hole solution in heterotic string theory,” *Phys. Rev. Lett.* **69** (1992), 1006-1009 doi:10.1103/PhysRevLett.69.1006 [arXiv:hep-th/9204046 [hep-th]].
- [28] I. Banerjee, B. Mandal and S. SenGupta, “Implications of Einstein–Maxwell dilaton–axion gravity from the black hole continuum spectrum,” *Mon. Not. Roy. Astron. Soc.* **500** (2020) no.1, 481-492 doi:10.1093/mnras/staa3232 [arXiv:2007.13980 [gr-qc]].
- [29] D. Wu, S. Q. Wu, P. Wu and H. Yu, “Aspects of the dyonic Kerr–Sen–AdS₄ black hole and its ultraspinning version,” *Phys. Rev. D* **103** (2021) no.4, 044014 doi:10.1103/PhysRevD.103.044014 [arXiv:2010.13518 [gr-qc]].
- [30] S. Jana and S. Kar, “Shadows in dyonic Kerr–Sen black holes,” *Phys. Rev. D* **108** (2023) no.4, 044008 doi:10.1103/PhysRevD.108.044008 [arXiv:2303.14513 [gr-qc]].
- [31] F. J. Tipler, “Rotating cylinders and the possibility of global causality violation,” *Phys. Rev. D* **9** (1974), 2203-2206 doi:10.1103/PhysRevD.9.2203
- [32] K. Gödel, “An Example of a New Type of Cosmological Solutions of Einstein’s Field Equations of Gravitation,” *Rev. Mod. Phys.* **21** (1949), 447-450 doi:10.1103/RevModPhys.21.447
- [33] J. R. Gott, III, “Closed timelike curves produced by pairs of moving cosmic strings: Exact solutions,” *Phys. Rev. Lett.* **66** (1991), 1126-1129 doi:10.1103/PhysRevLett.66.1126
- [34] J. A. Wheeler, “Geons,” *Phys. Rev.* **97**, 511-536 (1955) doi:10.1103/PhysRev.97.511
- [35] M. Alcubierre, “The Warp drive: Hyperfast travel within general relativity,” *Class. Quant. Grav.* **11**, L73-L77 (1994) doi:10.1088/0264-9381/11/5/001 [arXiv:gr-qc/0009013 [gr-qc]].
- [36] V. A. De Lorenci and E. S. Moreira, Jr., “Semi-classical backreaction around a nearly spinning cosmic string,” *Phys. Lett. B* **679**, 510-514 (2009) doi:10.1016/j.physletb.2009.08.019 [arXiv:0812.4516 [gr-qc]].
- [37] D. Sarma, M. Patgiri and F. U. Ahmed, *Gen. Rel. Grav.* **46** (2014), 1633 doi:10.1007/s10714-013-1633-7
- [38] F. Ahmed, B. Bikash Hazarika and D. Sarma, *Eur. Phys. J. Plus* **131** (2016) no.7, 230 doi:10.1140/epjp/i2016-16230-4
- [39] S. Chandrasekhar, “The mathematical theory of black holes,” Clarendon Press, 1985, ISBN 978-019-85-0370-5
- [40] C. Barceló, J. E. Sánchez, G. García-Moreno and G. Jannes, “Chronology protection implementation in analogue gravity,” *Eur. Phys. J. C* **82**, no.4, 299 (2022) doi:10.1140/epjc/s10052-022-10275-3 [arXiv:2201.11072 [gr-qc]].
- [41] F. Fiorini, “Chronology Protection in f(T) Gravity: The Case of Gott’s Pair of Moving Cosmic Strings,” *Universe* **10**, no.1, 52 (2024) doi:10.3390/universe10010052 [arXiv:2212.08647 [gr-qc]].
- [42] J. Santos, M. J. Rebouças and A. F. F. Teixeira, “Homogeneous Gödel-type solutions in hybrid metric–Palatini gravity,” *Eur. Phys. J. C* **78**, no.7, 567 (2018) doi:10.1140/epjc/s10052-018-6025-4 [arXiv:1611.03985 [gr-qc]].
- [43] A. M. Silva, M. J. Rebouças and N. A. Lemos, “Violation of Causality in f(Q) Gravity,” [arXiv:2407.04750 [gr-qc]].
- [44] J. R. Nascimento, A. Y. Petrov, P. J. Pořfırio and R. N. da Silva, “Gödel-type solutions within the f(R, Q, P) gravity,” *Eur. Phys. J. C* **83**, no.4, 331 (2023) doi:10.1140/epjc/s10052-023-11521-y [arXiv:2302.09935 [gr-qc]].
- [45] H. Andreka, I. Nemeti and C. Wuthrich, “A Twist in the geometry of rotating black holes: Seeking the cause of acausality,” *Gen. Rel. Grav.* **40** (2008), 1809-1823 doi:10.1007/s10714-007-0577-1 [arXiv:0708.2324 [gr-qc]].
- [46] C. Bambi, “Introduction to General Relativity,” Springer, 2018, ISBN 978-981-13-1089-8, 978-981-13-1090-4 doi:10.1007/978-981-13-1090-4
- [47] W. W. Bell, *Special Functions for Scientists and Engineers*, Courier Corporation (2004).
- [48] W. H. Press and S. A. Teukolsky, “Perturbations of a Rotating Black Hole. II. Dynamical Stability of the Kerr Metric,” *Astrophys. J.* **185**, 649-674 (1973) doi:10.1086/152445
- [49] E. Berti, V. Cardoso and M. Casals, “Eigenvalues and

- eigenfunctions of spin-weighted spheroidal harmonics in four and higher dimensions,” *Phys. Rev. D* **73**, 024013 (2006) [erratum: *Phys. Rev. D* **73**, 109902 (2006)] doi:10.1103/PhysRevD.73.109902 [arXiv:gr-qc/0511111 [gr-qc]].
- [50] E. Berti, V. Cardoso and M. Casals, “Eigenvalues and eigenfunctions of spin-weighted spheroidal harmonics in four and higher dimensions,” *Phys. Rev. D* **73**, 024013 (2006) [erratum: *Phys. Rev. D* **73**, 109902 (2006)] doi:10.1103/PhysRevD.73.109902 [arXiv:gr-qc/0511111 [gr-qc]].
- [51] H. T. Cho, A. S. Cornell, J. Doukas and W. Naylor, “Asymptotic iteration method for spheroidal harmonics of higher-dimensional Kerr-(A)dS black holes,” *Phys. Rev. D* **80**, 064022 (2009) doi:10.1103/PhysRevD.80.064022 [arXiv:0904.1867 [gr-qc]].
- [52] H. Suzuki, E. Takasugi and H. Umetsu, *Prog. Theor. Phys.* **100**, 491-505 (1998) doi:10.1143/PTP.100.491 [arXiv:gr-qc/9805064 [gr-qc]].
- [53] A. Das, *Field Theory: A Path Integral Approach* (2nd Edition), World Scientific Publishing Company (2006).
- [54] B. M. Karanov, V. P. Krainov *Field Theory: A Path Integral Approach* (2nd Edition), World Scientific Publishing Company (2006).
- [55] R. G. Daghigh, M. D. Green and J. C. Morey, “Calculating quasinormal modes of Schwarzschild anti-de Sitter black holes using the continued fraction method,” *Phys. Rev. D* **107**, no.2, 024023 (2023) doi:10.1103/PhysRevD.107.024023 [arXiv:2209.09324 [gr-qc]].
- [56] Z. S. Moreira, H. C. D. Lima, Junior, L. C. B. Crispino and C. A. R. Herdeiro, “Quasinormal modes of a holonomy corrected Schwarzschild black hole,” *Phys. Rev. D* **107**, no.10, 104016 (2023) doi:10.1103/PhysRevD.107.104016 [arXiv:2302.14722 [gr-qc]].
- [57] A. Ronveaux, *Heun’s Differential Equations*, Clarendon Press (1995).
- [58] S. Albeverio, N. Elander, W. Everitt and P. Kurasov, *Operator Methods in Ordinary and Partial Differential Equations: S. Kovalevsky Symposium*, University of Stockholm, June 2000, Birkhäuser Basel (2012).
- [59] S. Slavianov and W. Lay, *Special Functions: A Unified Theory Based on Singularities*, Oxford University Press (2000).
- [60] C. Chen and J. Jing, “Radiation fluxes of gravitational, electromagnetic, and scalar perturbations in type-D black holes: an exact approach,” *JCAP* **11** (2023), 070 doi:10.1088/1475-7516/2023/11/070 [arXiv:2307.14616 [gr-qc]].

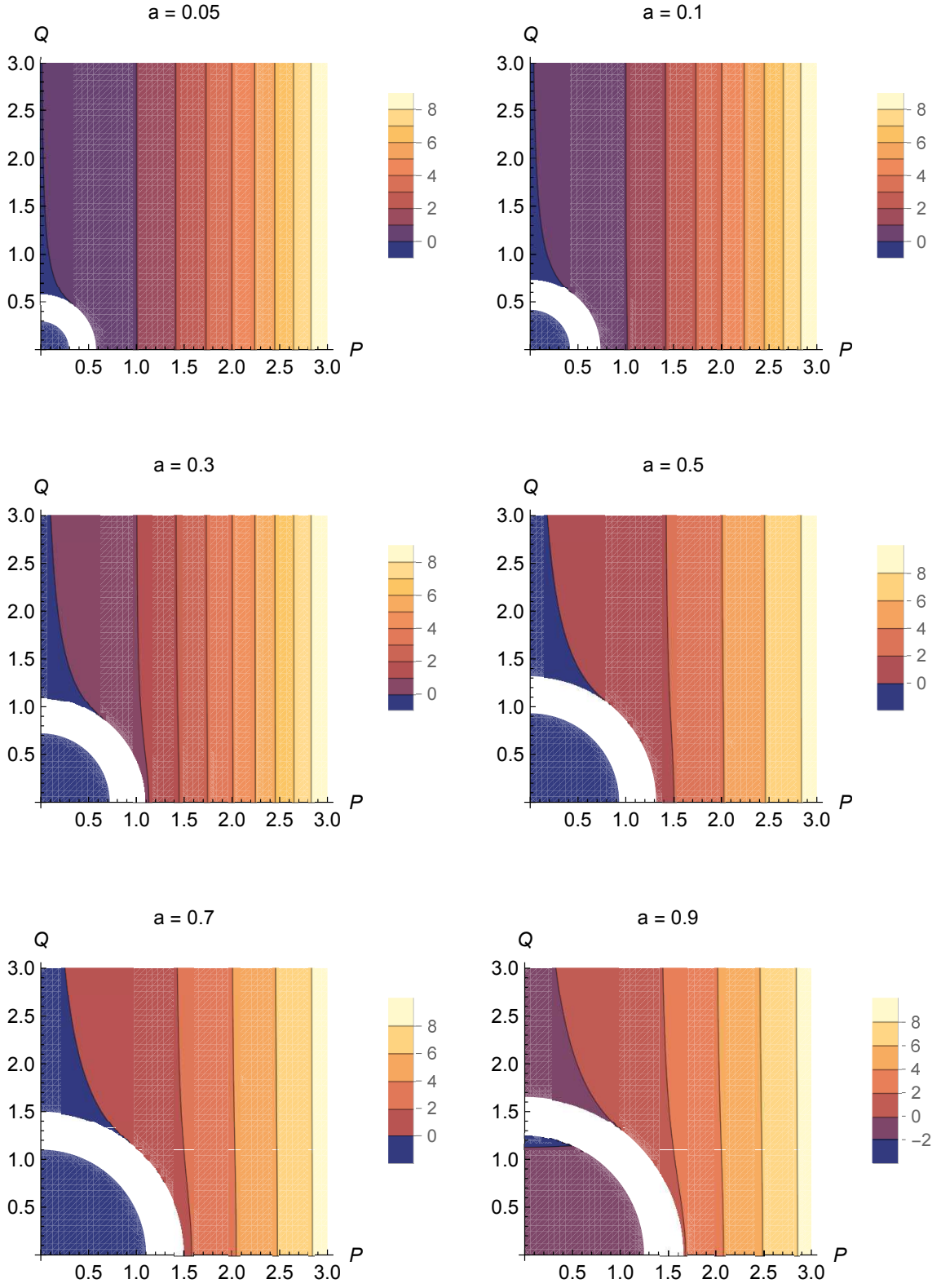


FIG. 1: Contour plot of the first boundary (r_1) of CTC regions.

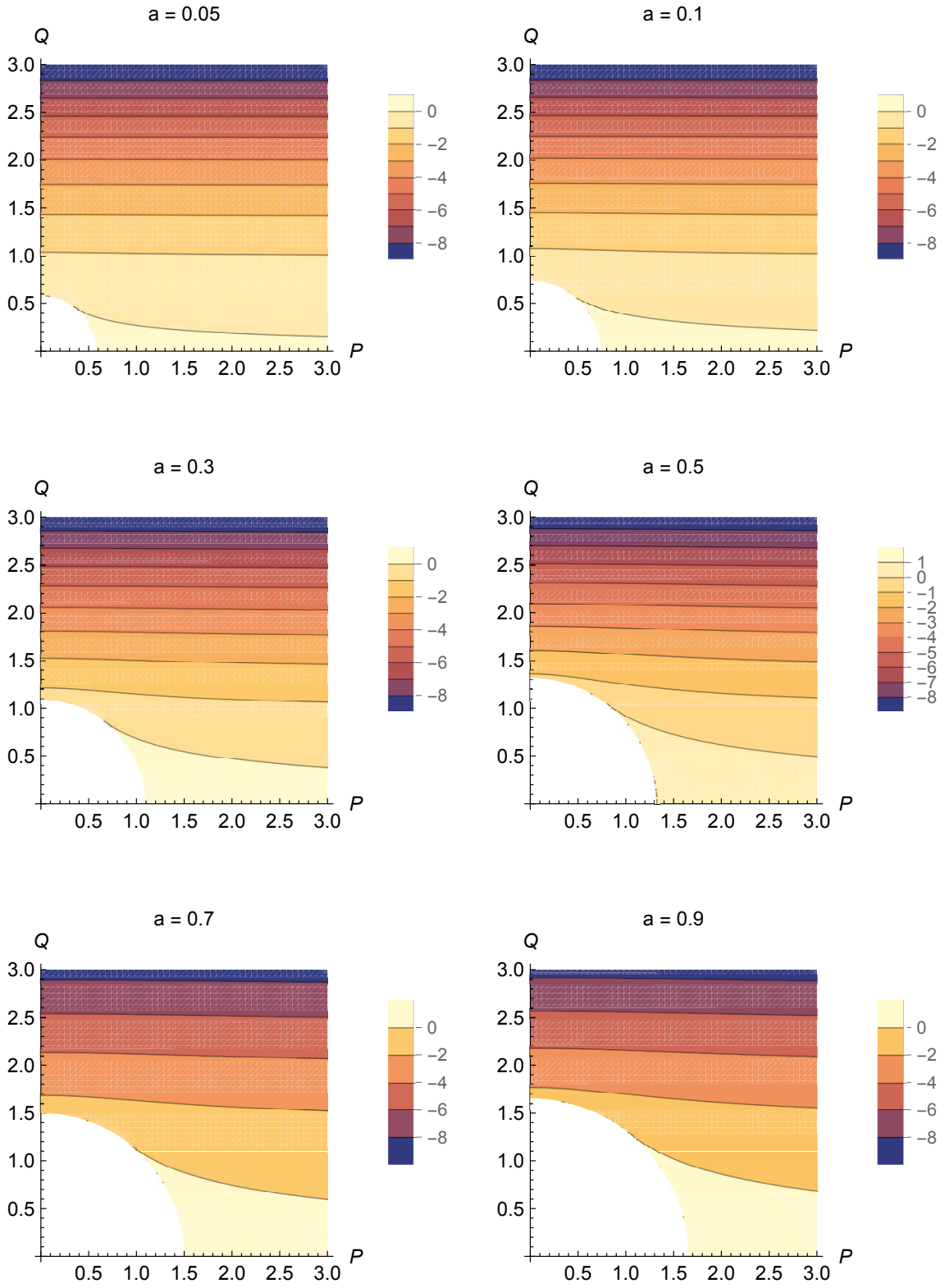


FIG. 2: Contour plot of the second boundary (r_2) of CTC regions.

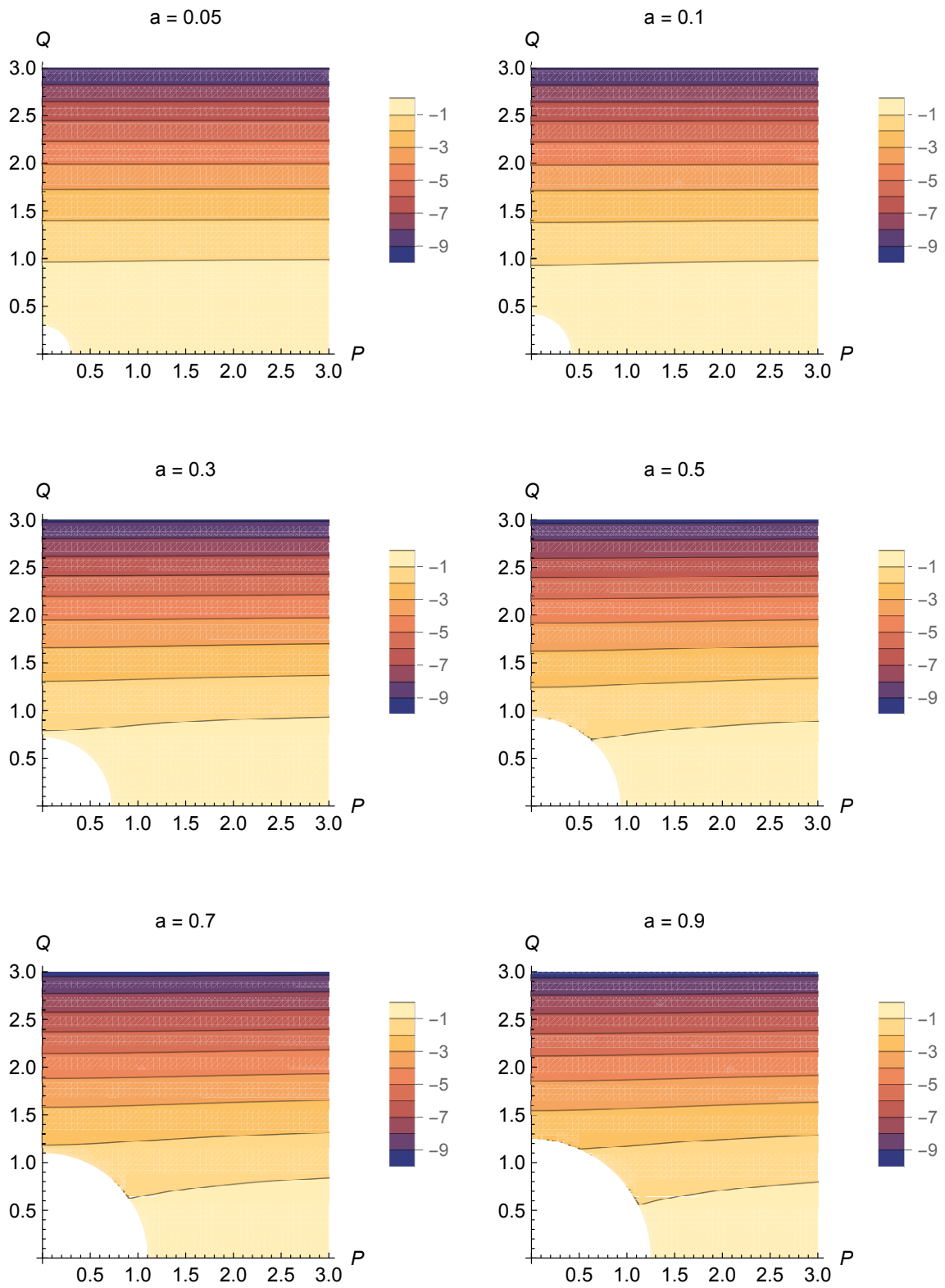


FIG. 3: Contour plot of the third boundary (r_3) of CTC regions.

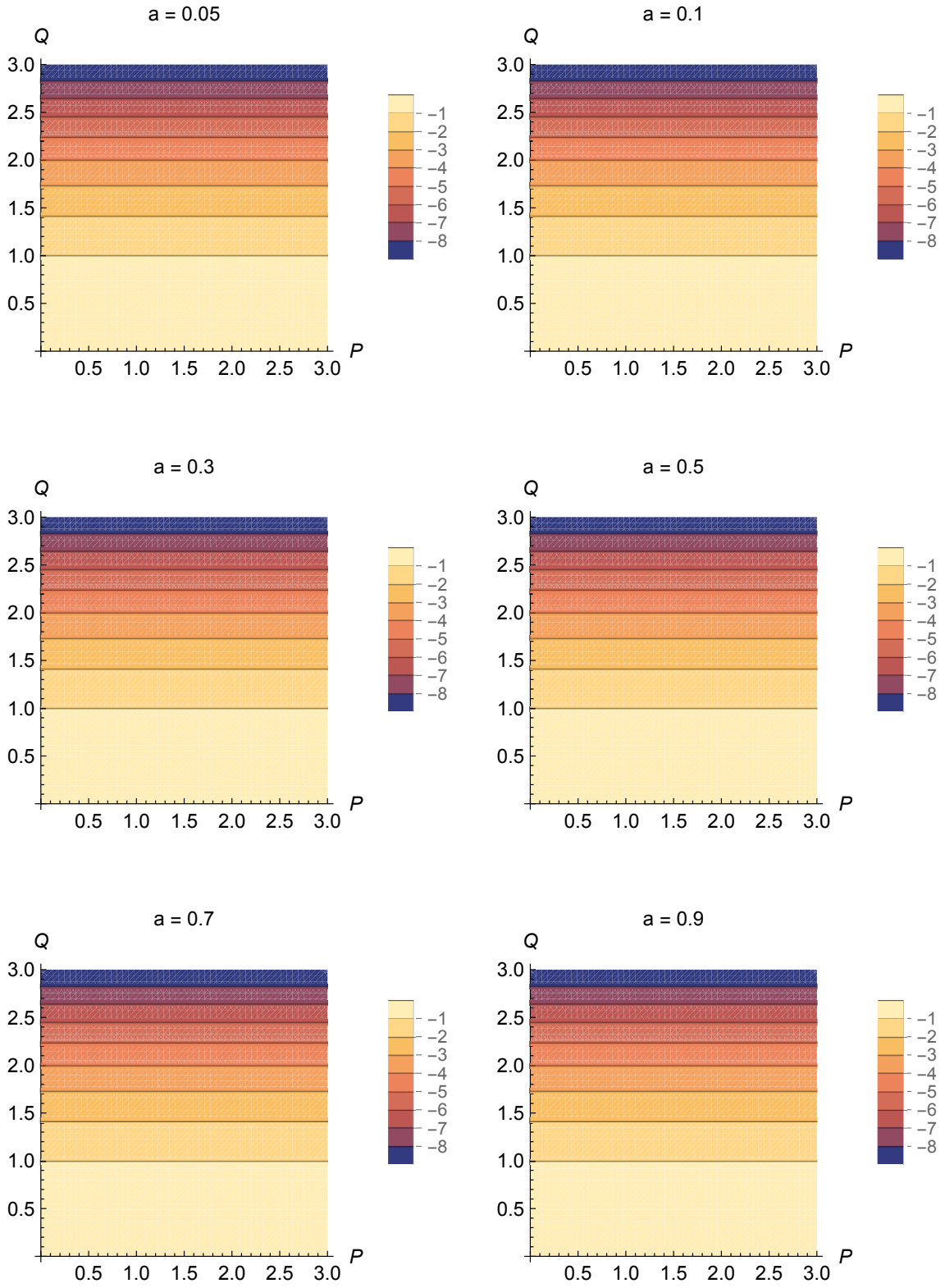


FIG. 4: Contour plot of the fourth boundary (r_m) of CTC regions.

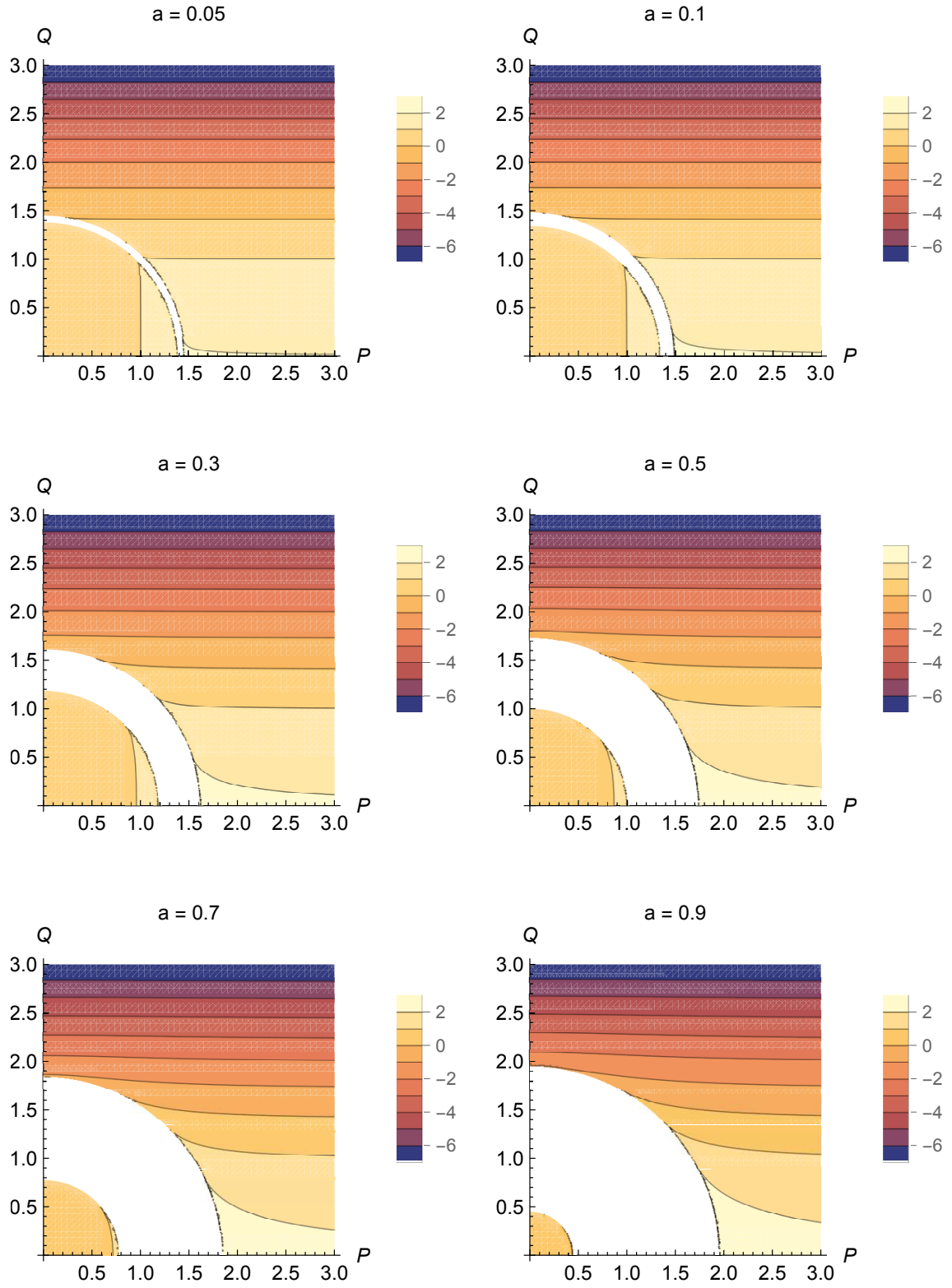


FIG. 5: Contour plot of the inner horizon (r_-).

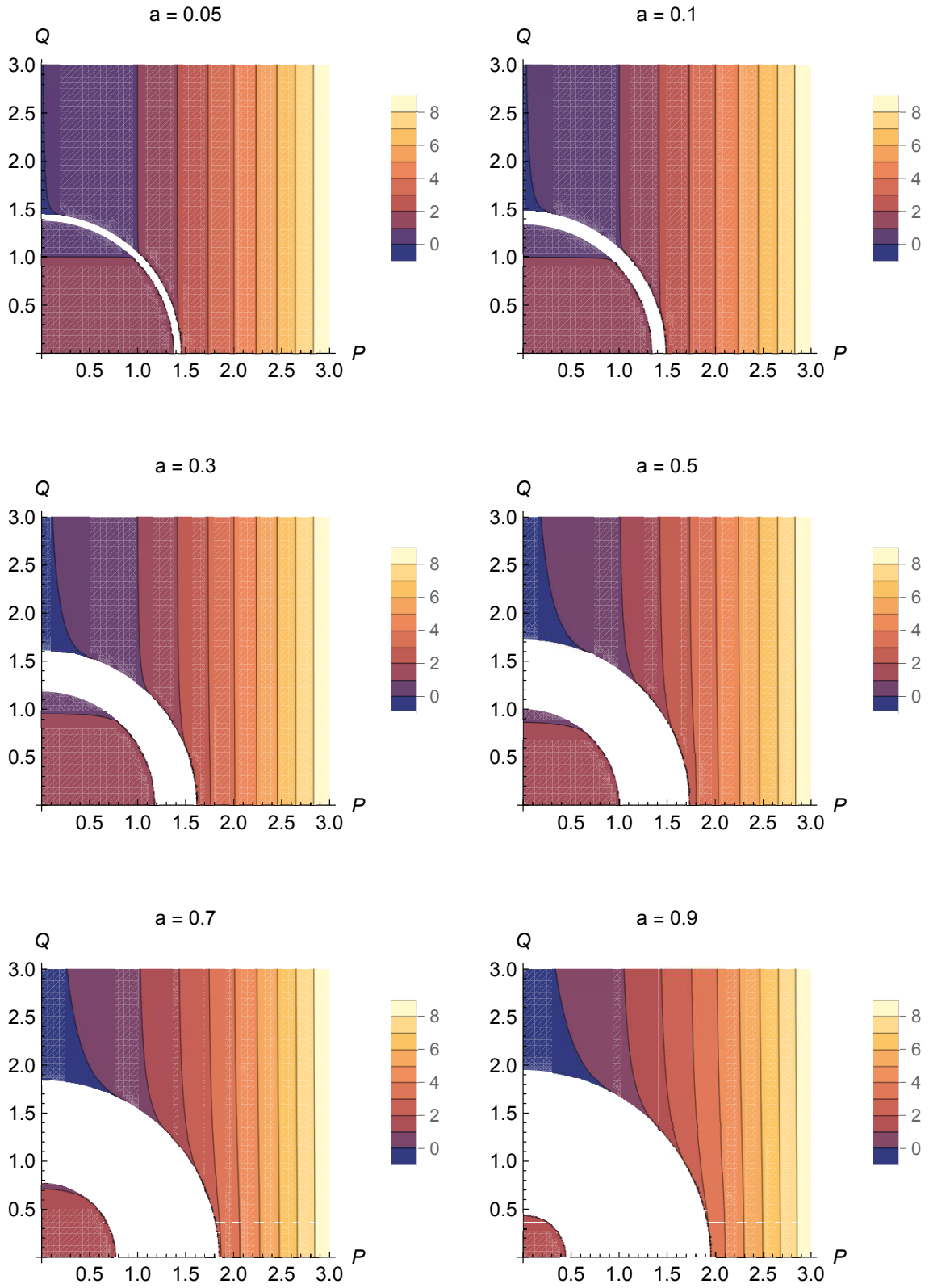
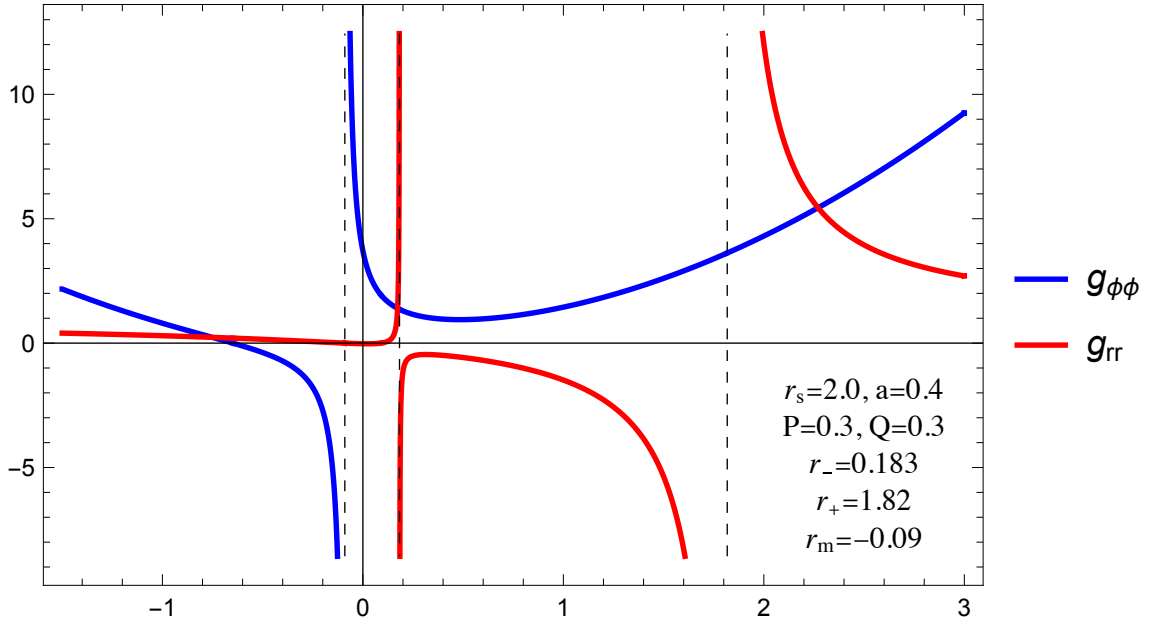
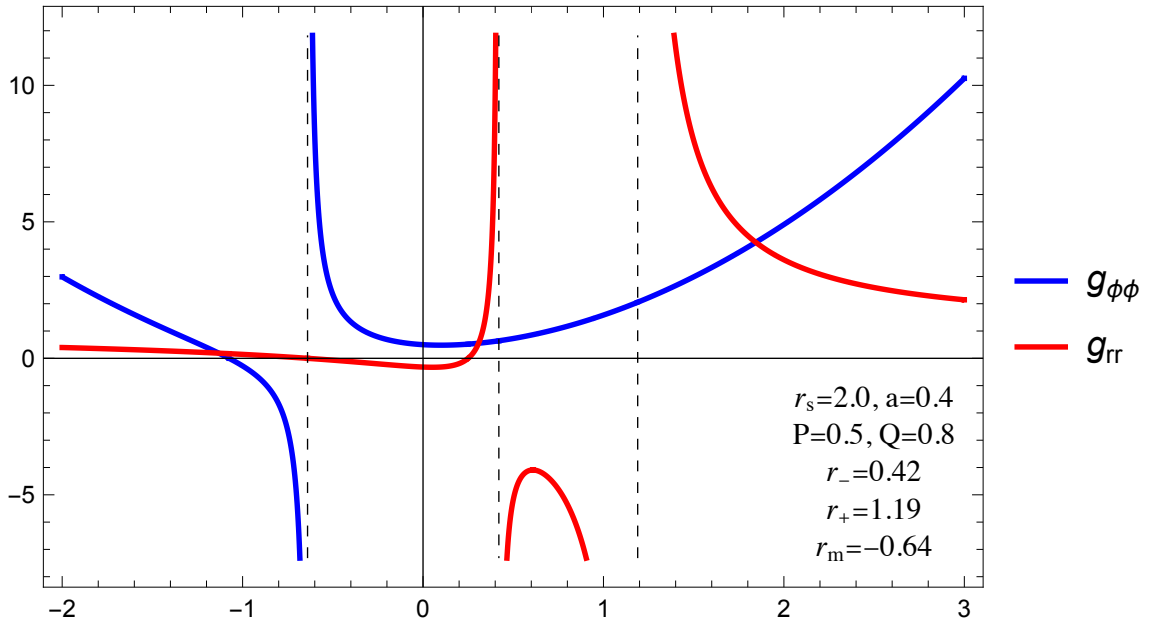
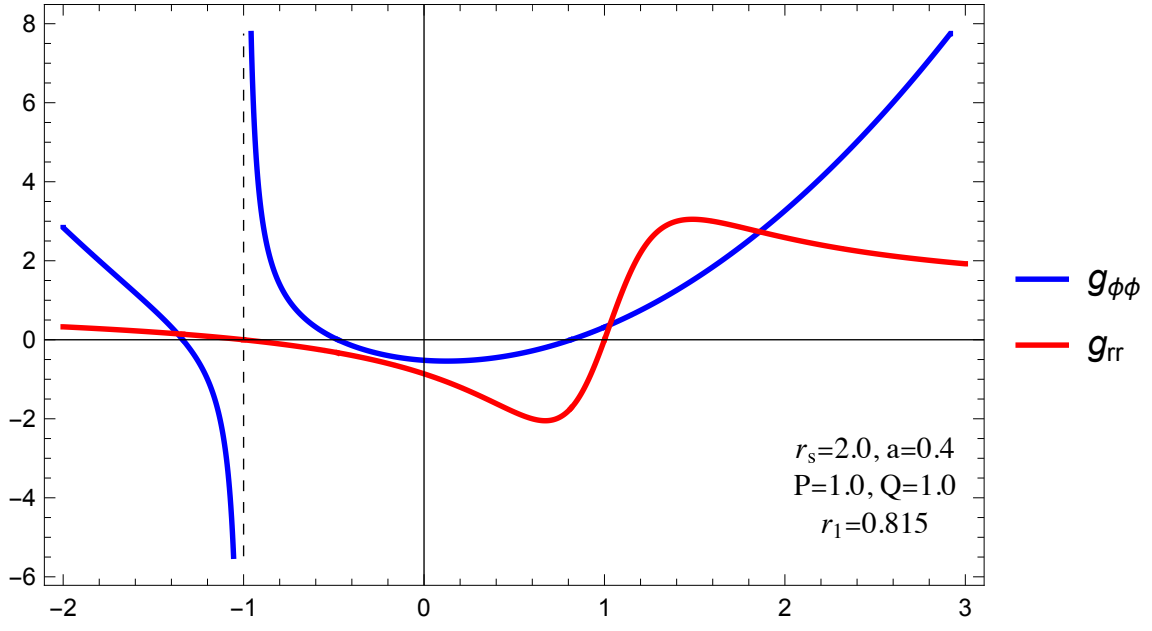
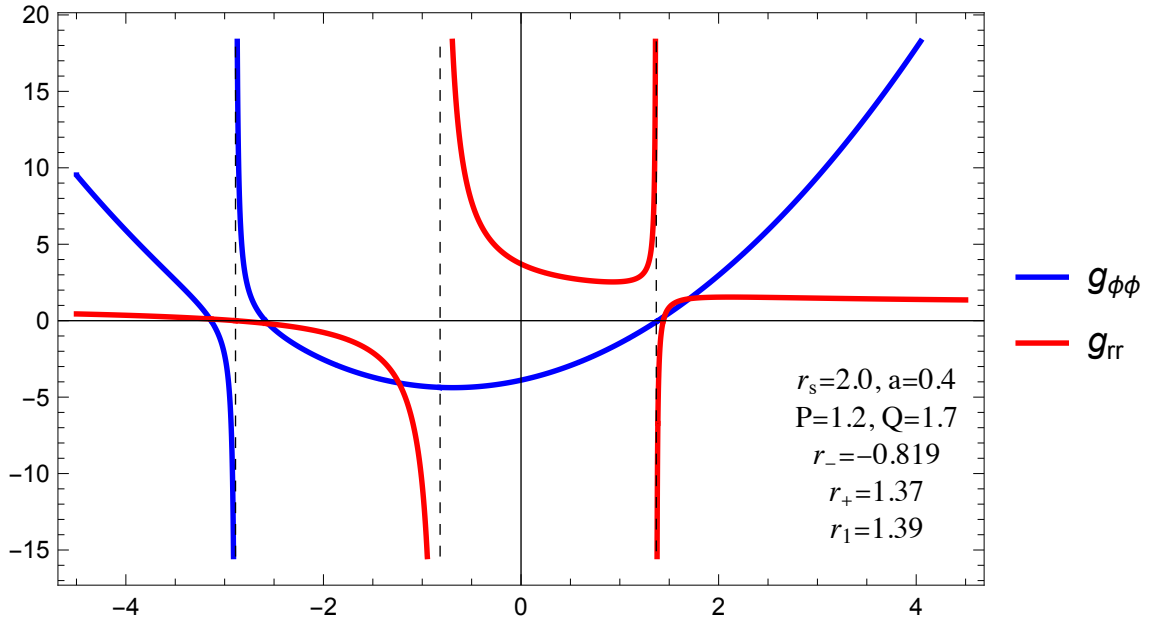
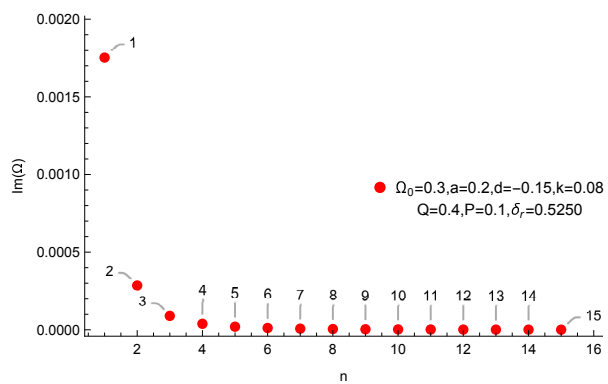
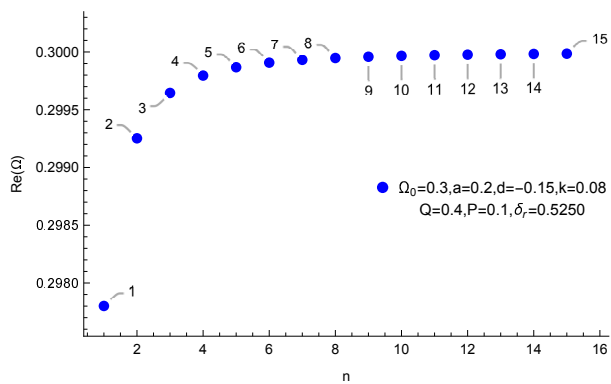
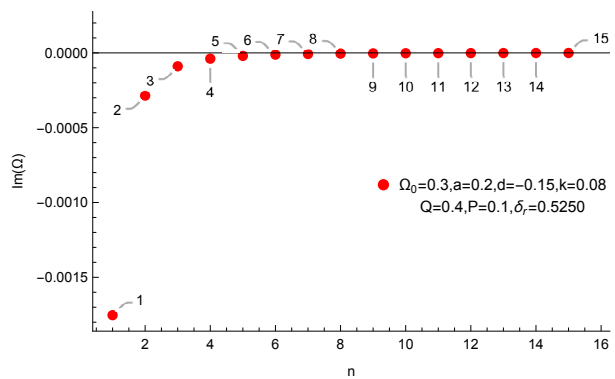
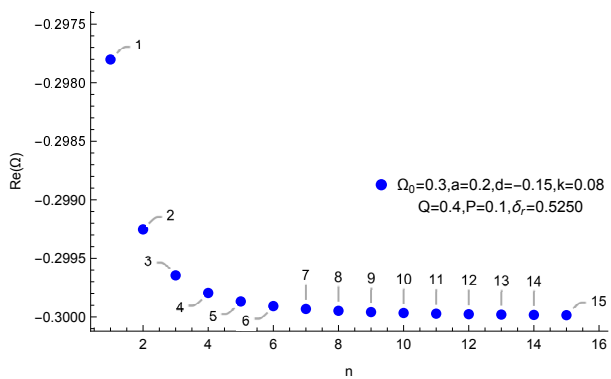
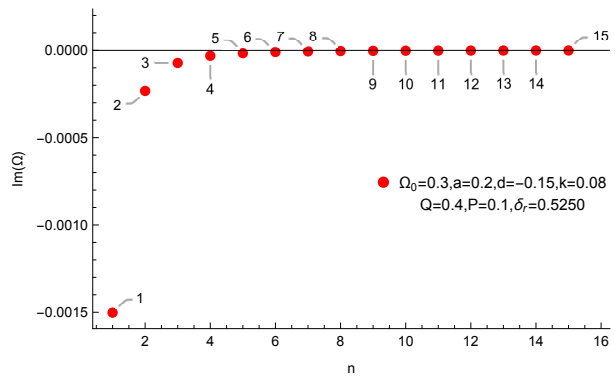
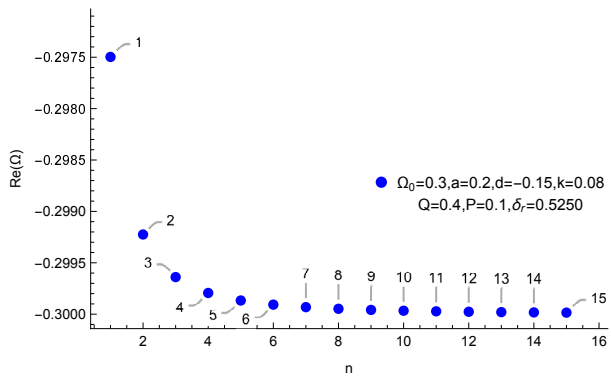
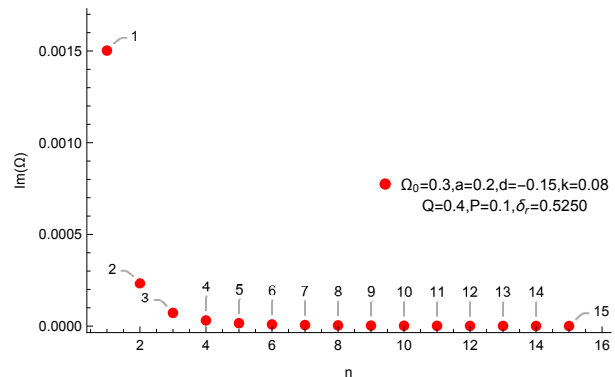
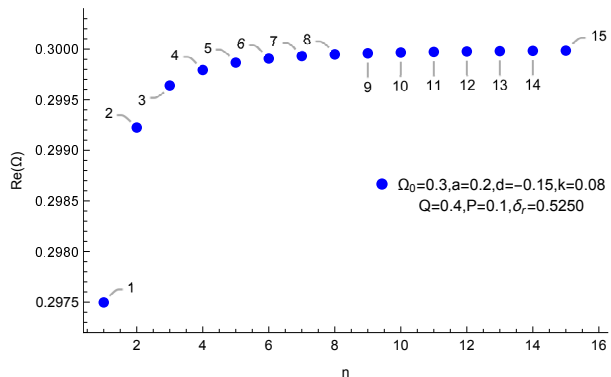


FIG. 6: Contour plot of the outer horizon (r_+).

FIG. 7: Plot of g_{rr} and $g_{\phi\phi}$ for very small-charge caseFIG. 8: Plot of g_{rr} and $g_{\phi\phi}$ for small-charge case

FIG. 9: Plot of g_{rr} and $g_{\phi\phi}$ for moderate charge caseFIG. 10: Plot of g_{rr} and $g_{\phi\phi}$ for large-charge case

QNMs of $\alpha_+ \beta_+ \gamma_+$ modeQNMs of $\alpha_+ \beta_- \gamma_-$ modeQNMs of $\alpha_+ \beta_+ \gamma_-$ modeQNMs of $\alpha_+ \beta_- \gamma_+$ mode

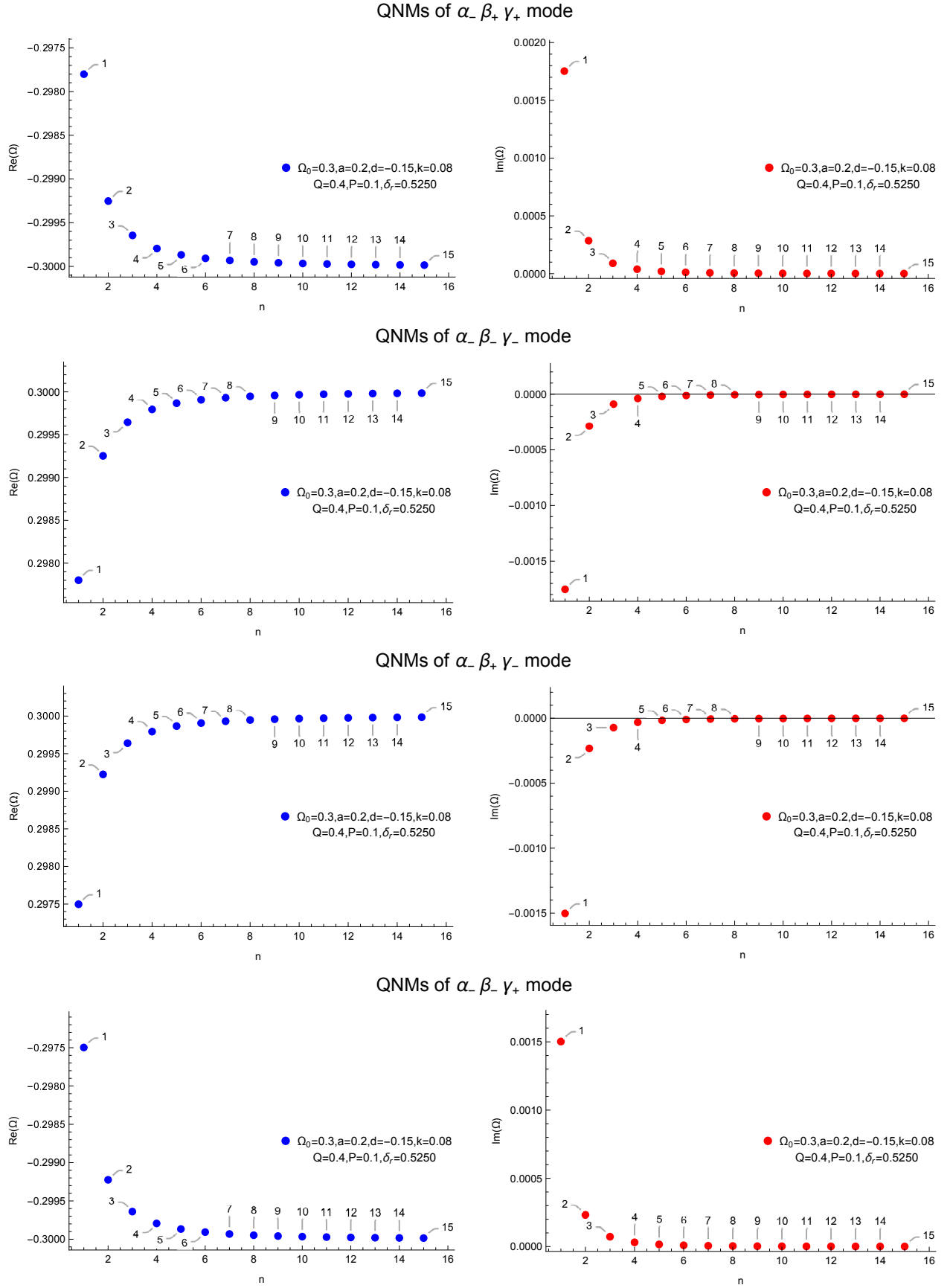


FIG. 11: Massive QNM's frequencies for all modes with $\Omega_0 = 0.3$.